İSTANBUL TECHNICAL UNIVERSITY ★ INSTITUTE OF SCIENCE AND TECHNOLOGY

DESIGN IMPROVEMENT OF TORQUE ROLL RESTRICTOR BRACKET

M.Sc. Thesis by
Pınar Feyza TOPRAK

Department : Mechanical Engineering

Programme : Otomotiv YL

FEBRUARY 2011

İSTANBUL TECHNICAL UNIVERSITY ★ INSTITUTE OF SCIENCE AND TECHNOLOGY

DESIGN IMPROVEMENT OF TORQUE ROLL RESTRICTOR BRACKET

M.Sc. Thesis by
Pınar Feyza TOPRAK
(503071724)

Date of submission : **20 December 2010**
Date of defence examination: **02 February 2011**

Supervisor (Chairman) : **Prof. Dr. Murat EREKE (ITU)**
Members of the Examining Committee : **Prof. Dr. Ahmet GÜNEY (ITU)**
Prof. Dr. İrfan YAVAŞLIOL (YTU)

FEBRUARY 2011

İSTANBUL TEKNİK ÜNİVERSİTESİ ★ FEN BİLİMLERİ ENSTİTÜSÜ

ŞANZIMAN ASKI SALINCAK BRAKETİNİN TASARIMININ İYİLEŞTİRİLMESİ

YÜKSEK LİSANS TEZİ

Pınar Feyza TOPRAK
(503071724)

Tezin Enstitüye Verildiği Tarih : 20 Aralık 2010
Tezin Savunulduğu Tarih : 02 Şubat 2011

Tez Danışmanı : Prof. Dr. Murat EREKE (İTÜ)
Diğer Jüri Üyeleri : Prof. Dr. Ahmet GÜNEY (ITU)
Prof. Dr. İrfan YAVAŞLIOL (YTU)

ŞUBAT 2011

FOREWORD

I would like to express my deep appreciation and thanks for my advisor Prof. Dr. Murat EREKE. This work is supported by ITU Institute of Science and Technology.

This study is supported by Ford Otosan A.Ş. and Kırpart A.Ş. I would like to thank my supervisor Ahmet TURAN for his great support, Prof. Dr. Ata MUĞAN, PhD Umud Esat ÖZTÜRK and Tufan ULUDAĞ for their supports in terms of technical information.

Last but not least, I would like to thank my family for their encouragement and assistance over my life.

December 2010

Pınar Feyza Toprak

Mechanical Engineer

TABLE OF CONTENTS

Page

ABBREVIATIONS

DIN : Deutches Institut für Normung
DV : Design Verification
FWD : Front Wheel Drive
SAE : Society of Automotive Engineers
TRR : Torque Roll Restrictor
CAE : Computer Aided Engineering
FEM : Finite Element Model
FEA : Finite Element Analysis
P/T : Powertrain
NVH : Noise, Vibration & Harshness
ASTM : American Society for Testing and Materials
EN : Europäische Norm
WOT : Wide Open Throttle
S/N : Stress vs. Number of cycles
UTS : Ultimate Tensile Stress

LIST OF TABLES

Page

LIST OF FIGURES

Page

LIST OF SYMBOLS

S_a, S_{Nf}	: Allowable stress
Nf	: Number of cycle
C	: Material Elasticity Matrix
E	: Modulus of Elasticity
G	: Modulus of Rigidity
F_e	: Force vector
K_e	: Element stiffness matrix
δ_e	: Displacement vector
σ	: Principle Stress
σmax	: Maximum Principle Stress
σmin	: Minimum Principle Stress
σequiv	: Equivalent Principle Stress
σ_x	: x-direction normal stress
σ_y	: **y**-direction normal stress
σ_z	: z-direction normal stress
τ_{xy} , τ_{yx}	: xy-plane shear stress
τ_{yz} , τ_{zy}	: **yz**-plane shear stress
τ_{xz} , τ_{xz}	: xz-plane shear stress
ε	: Strain
ε_x	: Strain in x direction
ε_y	: Strain in y direction
ε_z	: Strain in z direction
v	: Poisson's ratio
γ_{xy}	: Strain in xy plane
γ_{yz}	: Strain in yz plane
γ_{zx}	: Strain in zx plane
$F_{1,3,5}$	: Force vectors in horizontal direction
$F_{2,4,6}$	: Force vectors in vertical direction
$u_{1,2,3}$	: Unit vectors for horizontal direction forces
$v_{1,2,3}$	: Unit vectors for vertical direction forces

DESIGN IMPROVEMENT FOR TORQUE ROLL RESTRICTOR BRACKET

SUMMARY

In this thesis, failures on the torque roll restrictor (TRR) bracket used in Ford vehicles are investigated. Main reasons of failures are discussed and problem is solved by improving TRR bracket design.

To simulate the real road condition of the vehicle, vehicle durability test, driveline impact test and comparison oriented abuse & static tests are performed with the new supplier TRR bracket designs. Modifications on increasing radii & thickness of supports are the proposals for improvement. Several Finite Element Analyses were performed for each proposal. The results of the analyses were compared with the vehicle and component test results, which were performed during TRR bracket improvement studies.

Beside TRR bracket design improvement studies, material properties, porosity and hardness studies were performed in order to reveal the effects of the parameters on bracket fatigue and static strength performances according to change of supplier.

Static analyses with static and equivalent dynamic loads considering the condition of the maximum vehicle gross weight effect on the TRR bracket transferred from transmission to the roll restrictor mount were performed using finite element software. The results of the analysis were compared with the results of the tests.

In addition to design improvement of the TRR bracket, weight optimization was performed with correlated Finite Element model, as a next step of the study.

ŞANZIMAN ASKI SALINCAK BRAKETİNİN TASARIMININ İYİLEŞTİRİLMESİ

ÖZET

Bu çalışmada, Ford araçlarında kullanılan şanzıman askı salıncak takozlarında görülen kırılma ve çatlama hataları incelenmiştir. Sorunun kök sebepleri üzerinde durulmuş, takoz parçasının tasarım iyilemesi ile problemin çözümüne çalışılmıştır.

Mevcut tasarım şanzıman askı salıncak takozlarıyla yeni imalatçı ile tasarım iyilemesi yapılmış takozları, gerçek yol koşulları altında çalışma durumuna temsilen araç dayanıklılık testleri ve karşılaştırma amaçlı yorulma testleri tamamlanmıştır. Şanzıman askı salıncak takozundaki feder kalınlığı ve yarıçaplarını arttırma, iyileştirme için sunulan önerilerdir. Her bir öneri için çeşitli sonlu eleman analizleri yapılmıştır. Araç ve yorulma testlerin sonuçları, tasarım iyileştirme çalışmaları sırasında yapılan analizler ile karşılaştırılmıştır.

Şanzıman askı salıncak takozları tasarım iyileştirme çalışmalarına ilaveten, imalatçı değişiminden kaynaklanan, yorulma ve statik dayanım performansında etkili olabilecek malzeme özellikleri, dayanım ve gözeneklilik çalışmaları yapılmıştır.

Analizler statik ve dinamik yükler ile, sonlu elemanlar yöntemi ile aracın kendi ağırlığının maksimum düzeydeki etkisi ve şanzımandan askı salıncak ayağına iletilen yükün etkisi dikkate alınmak suretiyle sonlu elemanlar paket programı kullanılarak yapılmıştır. Analiz sonuçları, deneysel sonuçlar ile karşılaştırılmıştır.

Tasarı iyilemesinin yanında, testlerle doğrulanmış sonlu elemanlar modeli ile ağırlık optimizasyonu da, bir sonraki aşama çalışması olarak yürütülmüştür.

1. INTRODUCTION

Vehicle tests are performed at Ford vehicle test centre, which is Lommel Proving Ground, and abuse tests are performed at Ford OTOSAN Gölcük Plant. After that, TRR bracket will be modelled and FEA will be performed. The aim is to correlate the FEA model according to exact test results and prove accuracy of the model with further rig test. Finally, TRR bracket design improvement should be completed by FEA analysis, without performing any further vehicle test. This will provide Ford Motor Company significant cost saving by eliminating testing and engineering costs also mentioned by Dubensky (1986), that using CAE tools provide %27 time saving and %32 cost saving.

1.1 Background to study

Physically, the powerplant mount system consists of all the mounts, roll restrictors and dampers, all of the associated off-powerplant brackets, and any adapter brackets. The powertrain mounting system of a vehicle provides to support and locate the powerplant assembly, control/restrict movement of the powerplant assembly, to isolate the powerplant assembly for NVH, damp suspension inputs to body when acting as an auxiliary mass damper to absorb road inputs and reacting powerplant output torque and dynamic load inputs as the primary functions.

The function of the mounting system is to support powerplant weight, control gross motion under torque, and isolate P/T vibration inputs at all frequencies. These functions are carried out by two broad functional categories of elastomers: Base Mounts, and Roll Restrictors.

Roll Restrictors are defined as those mounting elements that perform the task of reacting high mean torque as well as isolate the vibration of the powerplant at high torque. The loads are transferred through the roll restrictor bracket to body side of vehicle. Therefore, in design of the roll restrictor bracket, vibration and durability should be in to consideration. In this study, only durability side will be important due to the slight change on bracket weight.

Design for durability should focus on the yield strength and fatigue strength of bracket. To this end, maximum loads that may produce stresses close to yield stress and continuous loads that may produce fatigue failure should be considered. These loads are typically given to the mount supplier to design for durability using analytical methods like FEA.

The magnitude of the maximum load is dependent upon vehicle structure, engine mount design, tire pressure, suspension, and powerplant. The mount system should be designed to withstand the maximum loads produced by the vehicle in the selected road load and special event testing. Mounts should be designed to prevent tensile yield at the maximum vehicle load inputs with a 10 percent design safety factor. In preliminary design work, before prototype vehicle road load data is available, the ultimate loads should be estimated from the test data of similar configuration and weight vehicles.

Actual mount loads can only be determined through the use of instrumented vehicles. Each mount's vertical, lateral, and longitudinal loads (it is desirable to measure accelerations also), and operating temperature, are measured and recorded. The road load data is reported in histogram form, load magnitude vs. number of occurrence, for the durability test route selected. Loads for special events such as curb impacts and chuckholes are reported in table form. Stress analysis on the design is then carried out using CAE or other standard calculations. In addition, load estimates of this type should be adjusted for differences in weight, suspension compliance, and tire size. In any case, upfront mount loads used for design should be representative of the loads used for design verification downstream as outlined in P/T Mount System Design Guideline (2004).

Fatigue is failure under repeated loads. The subsystem (both rubber and metal components) and its attachments must be designed to withstand the fatigue loading produced by the applicable Real World Usage Profile. In preliminary design work, before vehicles road load data are available, the road loads must be estimated from test data for similar configuration and weight vehicles or from correlated analytical models. The primary inputs to component life prediction with analytical techniques are: (1) a set of material properties related to cyclic deformation and (2) a loading time history of the component. The service loads of a component are derived experimentally through durability road routes or analytically/semi-analytically simulating the durability road inputs. Stress or strain spectra at critical locations are then determined by use of specialized computer programs and FEA.

2. THEORY OF FINITE ELEMENT ANALYSIS AND DURABILITY LIFE ESTIMATION

2.1 Background of Finite Element Analysis Theory

To obtain solutions to the differential equations for various physical and non-physical problems, the finite element method that is a numerical analysis technique used by engineers, scientists, and mathematicians.

The underlying premise of the finite element method is dividing a complicated domain to a series of smaller regions in which the differential equations are approximately solved. For each region, the set of equations are built to determine behaviour over the entire problem.

The domain is divided finite number of element as a region in a process that called as discretization. These elements are connected each other with nodes as a point. The process requires that the solution for the common boundaries of adjacent elements is continuous.

As described by Kenneth et al. (1982), the finite element procedure can be reduced to a series of basic steps. These are discretization of the continuum (meshing), selection of interpolation functions (in most cases, a polynomial interpolation function is used), finding the element properties (the field variable in the domain of the element is approximated in terms of discrete values at the nodes), assembling the elements (the value of the field variable at a node must be the same for each element which shares that node), applying the boundary conditions, solving the system of equations (If the system of equations is linear, a Gaussian elimination or Cholesky decomposition algorithm can be used), making additional computations (includes the computation of principal stress, Von Misses stress, and strain energy in a structural analysis, if needed).

2.1.1 Basic concepts in three – dimensional linear elasticity for stress components

The state of stress can be denoted by the normal stresses σ_x, σ_y, σ_z and six components of shear stress. In a Cartesian coordinate system, these components are configured on an element of volume as shown in Figure 2.1:

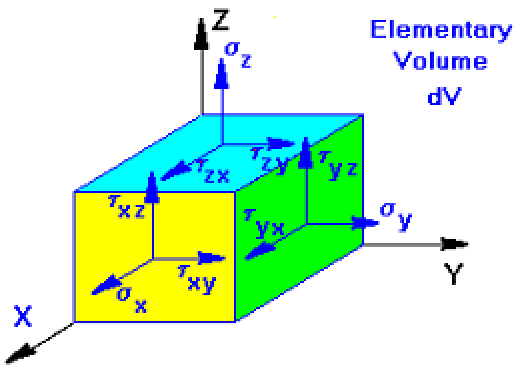

Figure 2.1 : Definition of Cartesian Stress Components.

By considering the equilibrium of forces as the element volume decreases in size, the symmetry of the shear stress components can be proven such that:

$$\tau_{yx} = \tau_{xy} \qquad \tau_{zy} = \tau_{yz} \qquad \tau_{zx} = \tau_{xz} \tag{2.1}$$

Hence, there are six unique components of stress represented in vector form:

$$\sigma = \begin{pmatrix} \sigma_x \\ \sigma_y \\ \sigma_z \\ \tau_{xy} \\ \tau_{yz} \\ \tau_{zx} \end{pmatrix} \tag{2.2}$$

The stresses are related to the strains through a constitutive law that is a function of the material properties.

The constitutive equations relate components of stress to the components of strain. In general, the relationship can be expressed as:

$$\sigma(x, y, z) = C \,.\, \varepsilon(x, y, z) \tag{2.3}$$

Where C is termed the material elasticity matrix.

For a general anisotropic material, the matrix C would have 36 terms. However, if only homogeneous and isotropic bodies are considered, then, a relatively simple matrix may be obtained. Homogeneous implies that the material properties are the same everywhere within the body, while isotropic implies that the material properties are identical in all directions.

Using Hooke's law gives the following relationships:

$$\varepsilon_x = \frac{\sigma_x}{E} - \nu \cdot \frac{\sigma_y}{E} - \nu \cdot \frac{\sigma_z}{E} \qquad \gamma_{xy} = \frac{1}{G} \cdot \tau_{xy}$$

$$\varepsilon_y = \frac{\sigma_y}{E} - \nu \cdot \frac{\sigma_x}{E} - \nu \cdot \frac{\sigma_z}{E} \qquad \gamma_{yz} = \frac{1}{G} \cdot \tau_{yz} \qquad \textbf{(2.4)}$$

$$\varepsilon_z = \frac{\sigma_z}{E} - \nu \cdot \frac{\sigma_x}{E} - \nu \cdot \frac{\sigma_y}{E} \qquad \gamma_{zx} = \frac{1}{G} \cdot \tau_{zx}$$

where E is the modulus of elasticity, ν is Poisson's ratio, and G is the modulus of rigidity.

The latter constant may be expressed as:

$$G = \frac{E}{2 \cdot (1 + \nu)} \qquad \textbf{(2.5)}$$

Rewriting the normal strains of equation (2.5) in matrix form gives

$$\begin{pmatrix} \varepsilon_x \\ \varepsilon_y \\ \varepsilon_z \end{pmatrix} = \frac{1}{E} \cdot \begin{pmatrix} 1 & -\nu & -\nu \\ -\nu & 1 & -\nu \\ -\nu & -\nu & 1 \end{pmatrix} \cdot \begin{pmatrix} \sigma_x \\ \sigma_y \\ \sigma_z \end{pmatrix} \qquad \textbf{(2.6)}$$

Inverting the 3 x 3 matrix expresses the normal stress components in terms of the normal strains:

$$\begin{pmatrix} \sigma_x \\ \sigma_y \\ \sigma_z \end{pmatrix} = \frac{E}{(1 + \nu) \cdot (1 - 2 \cdot \nu)} \cdot \begin{pmatrix} 1 - \nu & \nu & \nu \\ \nu & 1 - \nu & \nu \\ \nu & \nu & 1 - \nu \end{pmatrix} \cdot \begin{pmatrix} \varepsilon_x \\ \varepsilon_y \\ \varepsilon_z \end{pmatrix} \qquad \textbf{(2.7)}$$

Combining the shear components of (2.4) with (2.7) yields the matrix C of equation (2.8):

$$C = \frac{E}{(1+\nu)\cdot(1-2\cdot\nu)}\cdot\begin{pmatrix} 1-\nu & \nu & \nu & 0 & 0 & 0 \\ \nu & 1-\nu & \nu & 0 & 0 & 0 \\ \nu & \nu & 1-\nu & 0 & 0 & 0 \\ 0 & 0 & 0 & \frac{1-2\cdot\nu}{2} & 0 & 0 \\ 0 & 0 & 0 & 0 & \frac{1-2\cdot\nu}{2} & 0 \\ 0 & 0 & 0 & 0 & 0 & \frac{1-2\cdot\nu}{2} \end{pmatrix} \qquad \textbf{(2.8)}$$

Observe that the C is symmetric and is a function of the modulus of elasticity and Poisson's ratio.

Other constitutive laws exist (for anisotropic bodies) that allow for different material properties in different directions.

In plane stress, the continuum is usually a thin structure such as a plate, and stresses normal to the plane are assumed to be negligible.

The non-zero components of stress and strain are:

$$\sigma = \begin{pmatrix} \sigma_x \\ \sigma_y \\ \tau_{xy} \end{pmatrix} \qquad \gamma = \begin{pmatrix} \varepsilon_x \\ \varepsilon_y \\ \gamma_{xy} \end{pmatrix} \qquad \textbf{(2.9)}$$

2.1.2 A triangular element in plane stress

In the previous section, the equations of three-dimensional linear elasticity were presented followed by a specialization to plane stress and plane strain problems. In this section, finite elements of elastic continua are developed as applied to two-dimensional problems of plane stress. The most geometrically versatile element and simplest of two-dimensional elements is the triangular element.

The derivation of the equations for the elastic triangular element dates back to 1956 in classic paper by Turner et al. (1956) referred to as the direct method; the derivation is used as a point of departure into more abstract concepts.

The element equations consider a typical triangular element of thickness, t, with the following forces and displacements at the nodes in Figure 2.2:

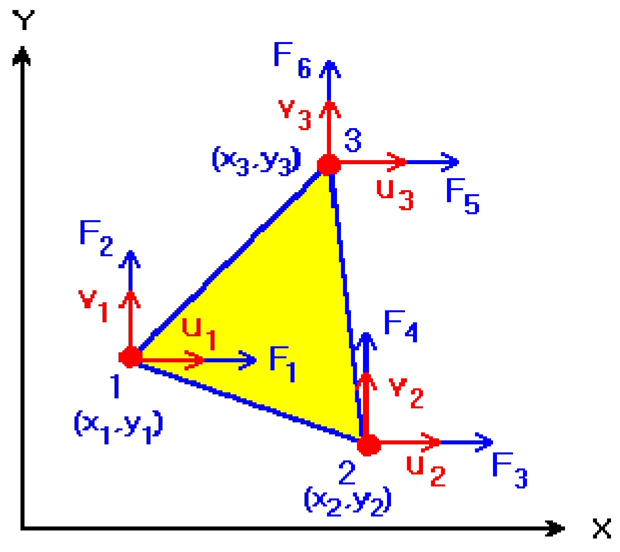

Figure 2.2 : Triangular element in plane stress.

The element above has two degrees of freedom per node that correspond to the horizontal and vertical components of displacement. There are a total of six degrees of freedom for the element. In matrix notation the force-displacement equations for the element become

$$K_e \cdot \delta_e = F_e \qquad \textbf{(2.10)}$$

where K_e is the element stiffness matrix and the displacement and force vectors are defined as

$$\delta_e = (\ u_1\ v_1\ u_2\ v_2\ u_3\ v_3\ )^T \qquad \textbf{(2.11)}$$

$$F_e = (\ F_1\ F_2\ F_3\ F_4\ F_5\ F_6\ )^T \qquad \textbf{(2.12)}$$

respectively.

The element stiffness matrix, K_e, will be determined using the direct method and the energy method. It will be shown that the direct model is the more intuitive method and can be applied most practically too simple element shapes. On the other hand, the energy method is a general formulation that allows the finite element method to extend beyond the realm of elasticity.

2.2 Theory of Optimization Method

In this study Altair OptiStruct has been used as an optimization tool. OptiStruct is a finite element and multi-body dynamics software which can be used to design and optimize structures and mechanical systems. OptiStruct uses the analysis capabilities of RADIOSS and MotionSolve to compute responses for optimization.

RADIOSS can be used to analyze a wide variety of design problems in which the structural and system behaviour can be simulated using finite element and multi-body dynamics analysis.

The analysis capabilities are comparable to those of other standard finite element and multi-body dynamics solvers. It uses the latest numerical formulations available and fast, and robust solver techniques.

MotionSolve provides a comprehensive set of elements to help one model and simulate an almost infinite variety of mechanical and mechatronic systems. These elements can be combined to model systems such as vehicles, hard disk drives, aircrafts, satellites, and robots. These systems can be analyzed for various performance criteria, such as motion, mechanical advantage, power requirements, vibration, stability, loading, efforts, interference, penetration, stress distribution, durability, and controllability.

Structural design tools include topology, topography, and free-size optimization. In this study, topology optimisation has been used.

In the formulation of design and optimization problems, the following responses can be applied as the objective or as constraints: compliance, frequency, volume, mass, moment of inertia, centre of gravity, displacement, velocity, acceleration, buckling factor, stress, strain, composite failure, force, synthetic response, and external (user defined) functions. In this study, linear static forces are applied and single points of contacts are used as constraints.

Topology, topography, size, and shape optimization can be combined in a general problem formulation.

2.2.1 Topology optimisation

Topology optimization generates an optimized material distribution for a set of loads and constraints within a given design space. The design space can be defined using shell or solid elements, or both. The classical topology optimization set up solving the minimum compliance problem, as well as the dual formulation with multiple constraints are available. Constraints on von Misses stress and buckling factor are available with limitations. Manufacturing constraints can be imposed using a minimum member size constraint, draw direction constraints, extrusion constraints, symmetry planes, pattern grouping, and pattern repetition.

Different solution sequences are available to compute structural responses. Solutions for optimization are: linear static analysis, normal modes analysis, linear buckling analysis, frequency response analysis using the modal method, and non-linear gap analysis.

Solutions that are not yet available for optimization are: frequency response analysis using the direct method, random response analysis, transient response analysis, thermal analysis, fluid-structure (acoustic) analysis, and fatigue analysis.

2.3 Theory of Durability Life Estimation

2.3.1 Background study for durability life estimation

Currently, proper fatigue design involves synthesis, analysis, and testing. Fatigue testing alone is not a proper fatigue design procedure, since it should be used for product durability determination, not for product development. Analysis alone is current fatigue limit.

Aichberger et al. (2007) show a graphical data of AlSi9Cu3 engine support bracket fatigue life assumption with FEMFAT local stress-life concept and local strain-life methods, in x-direction loading, in SAE 2007 Congress. As seen in the Figure 2.3 stress-life approach is giving a better results but it is not sufficient due to the surface boundary layer of an AlSi9Cu3 with die casting is pore-free due to the manufacturing process. Therefore, it would be more durable then nominal local life assumption.

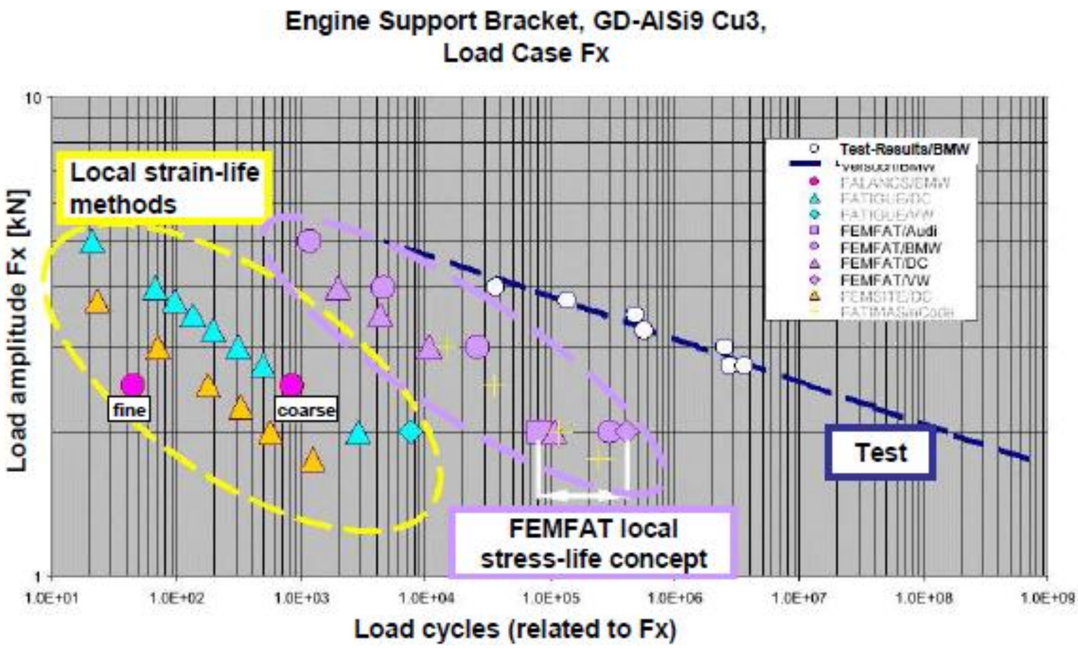

Figure 2.3 : Calculations with nominal material properties and testing results.

For life assumption from stress values approach, Basquin (1910) suggested a log-log straight line S/N relationship such that;

$$Sa \text{ or } S_{Nf} = A(N_f)^B \qquad \textbf{(2.13)}$$

Figure 2.4 illustrates the process for determining the maximum allowable stress limit when designing the component using CAE tools, as outlined in section 3 Figure 2.4 is a generic curve for aluminium alloys with a UTS of between 240-320 MPa. It represents the fatigue strength of a component composed of this material when subjected to repetitive / intermittent load cycling (+/- peak load). Due to the inherent nature/functionality of P/T mount system parts they must withstand cycling loads in addition to a simple static strength as indicated in Modelling, Analysis and Reporting Guidelines (Farrington et al., 2003).

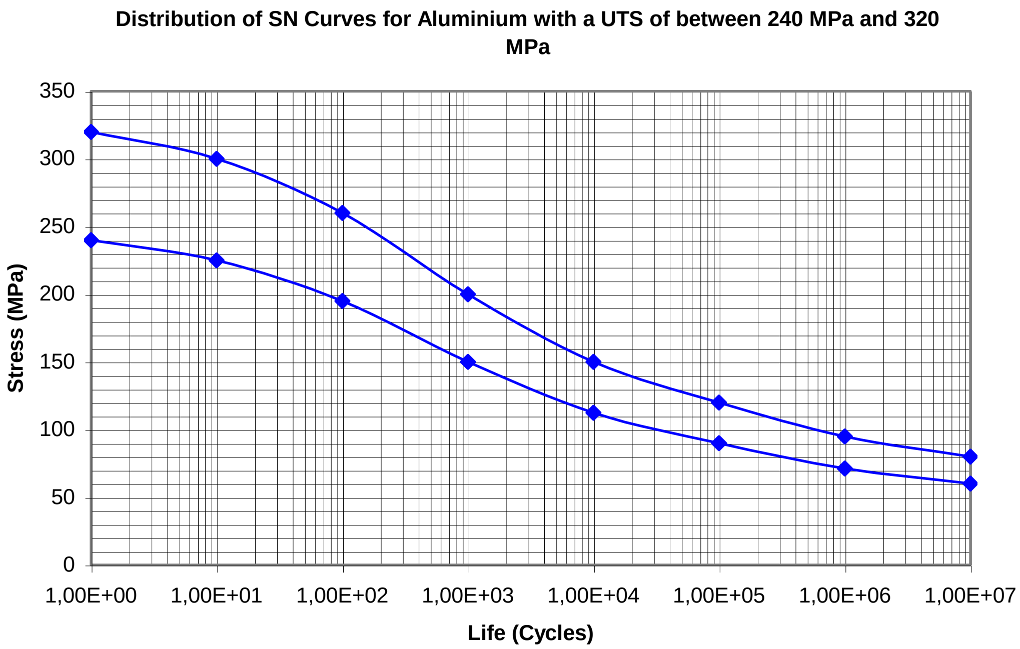

Figure 2.4 : Distribution of S/N Curves for Aluminium with a UTS of between 240 MPa and 320 MPa.

In this study, AlSi9Cu3(Fe) is used as a TRR bracket material whose UTS is changing between 240 - 320 MPa due to die casting manufacturing process effect. For the testing results and FEA results this effect will be considered.

2.3.2 Calculation of CAE predicted minimum life of the TRR bracket in rig condition

The test/CAE where correlation can be investigated here is the peak X load case – this would represent an event such as a very severe and unintentional stop impact (such that this would be one of the worst 100 such events in the life of a 95th percentile vehicle).

After all analysis done stress areas will be determined. Upon inspection it is judged that area one of them has the highest stresses, and so the maximum stress will be used with the numbers taken from that area. All of the remaining results are calculated in the same manner, in line with the Modelling, Analysis and Reporting Guidelines (Farrington et al., 2003).

There is two way to calculate stresses with respect to guideline in terms of reversibility and safety factors coming from mesh quality and selected order of elements. For the brittle material such as aluminium alloys ford guide line states that S/N curve would be used to determine life from stress level on part.

If the stress is not reversal before reading life from S/N curve some normalisation should be done on the results to find equivalence stress value. To normalise the minimum and maximum principle stresses. These values would be found with multiplying by 1.3 with read value from FEA results. After normalized values obtained the following formulation to be applied to gain equivalence stress:

$$\sigma equiv = 0.25*(3* \sigma max - \sigma min) \quad \textbf{(2.14)}$$

If one uses Von Misses values and system is reversible, than only non-homogeneity & surface finish, geometry variation and coarse order safety factors would be applied.

To allow for non-homogeneity and surface finish the safety factor is 1.1-1.2, to allow for component geometry variation safety factor is 1.1-1.2 and to factor for fine high order tetrahedral 1.1 safety factor should be applied to results.

3. TORQUE ROLL RESTRICTOR BRACKET DURABILITY ISSUE AND THE ASSOCIATED STUDIES

3.1 TRR Bracket Implementation History

For V227, Ford had supplied the initial defined TRR bracket from the same supplier of Ford Focus TRR bracket. In 2003, localization of supplier study for V227 was performed to gain effective part transportation. In that study, both suppliers' parts were tested back-to-back and parts were signed-off according to Ford TRR Bracket Engineering Specification (2004).

After the localization study, there is no change recorded on bracket design since 2003.

3.2 Definition of Failure Modes

The first step of this study is to reveal the reasons for the failure of the bracket. Due to the high warranty samples, cause effects are investigated. Cause effects might be due to insufficient clamp load of bolts caused by assembly wrong bolt torque value, supplier production process, material properties or wrong design parameters.

Before defining the failure modes, the warranty data (Figure 3.1) should be reviewed to understand the dimension of the failure mode.

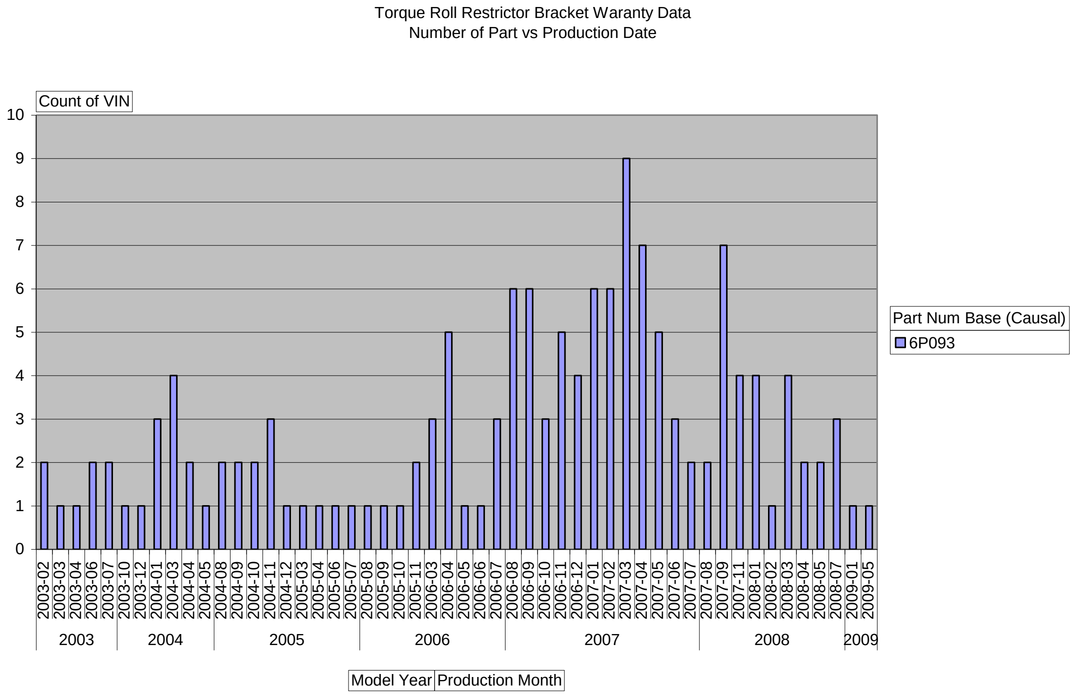

Figure 3.1 : Warranty data of TRR bracket that have been produced in between Feb2003 - May2009.

Ford warranty database (Figure 3.1) shows that the production line supplier produces the TRR bracket with 3.5 sigma value. In general, 3.5-4 sigma values are acceptable for automotive industries. However, Ford Otosan has a target to reach working with 6-sigma values with all components. Therefore, the aim is to improve TRR bracket part to 6-sigma value.

To define failure mode all steps should be investigated. Before deciding which failure mode causes to this effect, number of failed part vs. failure [km] range should be also discussed. As seen in Figure 3.2 most of the failure mode has occurred in low mileage. That means the failure mode is not due to the low stress safe-life fatigue but due to the high impact loads to fail before determined number of finite life cycle.

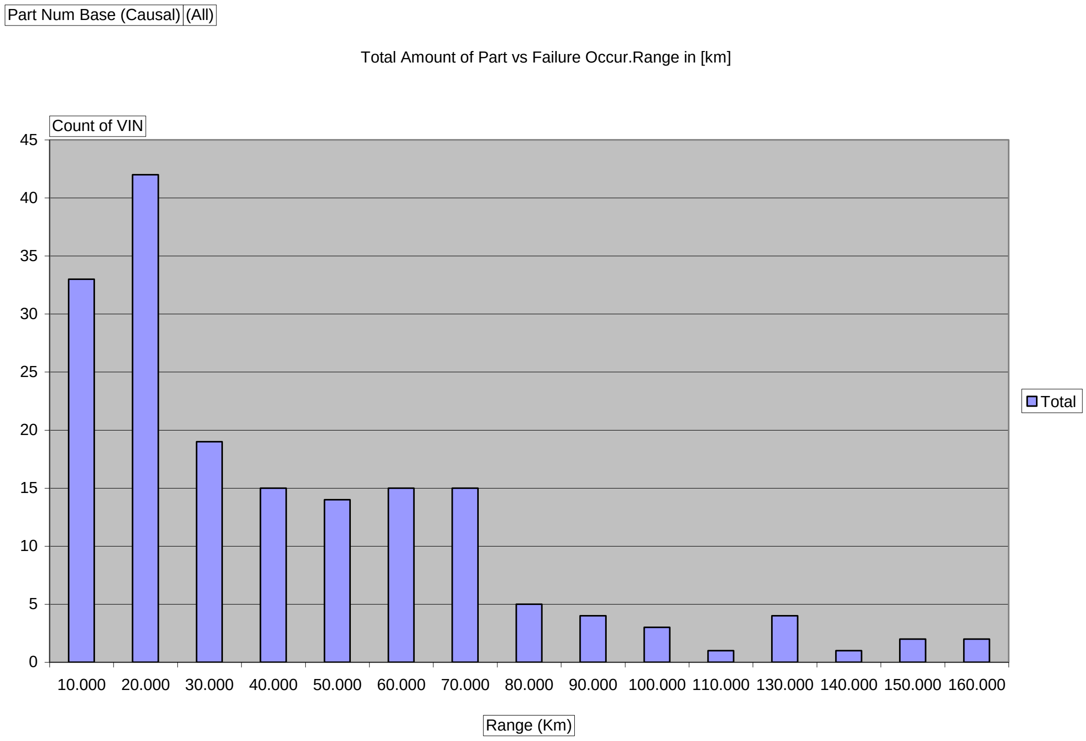

Figure 3.2 : Total amount of failed part vs. failure mileage range.

3.2.1 Assembly line bolt torque values

An impact-load failure mode can be due to the bolt torque loss. A standard hexagonal bolt approximate torque values are calculated by Norm (2007) with respect to nominal diameter, pitch, grade, and friction coefficient of threads of the bolt. For TRR system, all five-bolts used are M10 x 1.5 with grade 8.8 and their thread friction coefficients are given as nominal 0.20. For these values catalogue shows average value should be 53Nm. In assembly line, bolts are torqued to 47.5Nm ± 7.2Nm by computer controlled air wrench tool and if there is a missing and/or wrong-torqued bolt exist, that stops the line and gives an alarm (torque sequence process is shown in Figure 3.3).

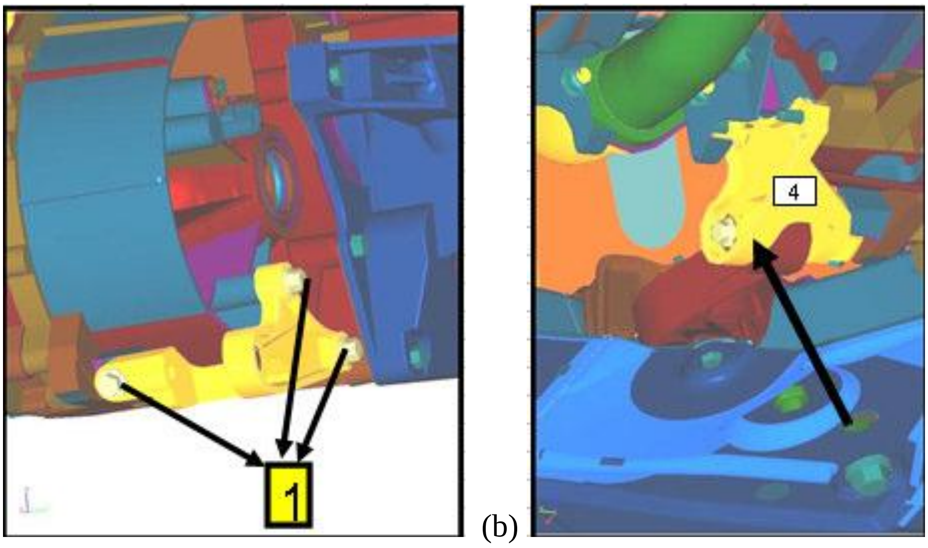

(a) (b)

Figure 3.3 : Process sequence of TRR bracket to (a) transmission and (b) the roll restrictor.

The torque values are in nominal values of standards and process controlled by computer safely (all data are saved in process report sheet that seen is Figure 3.4 as an example - no failure in the assembly line was detected so far).

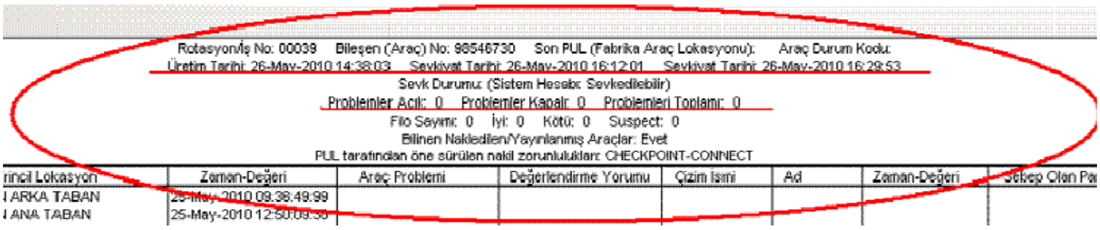

Rotasyon/İş No: 00039 Bileşen (Araç) No: 98546730 Son PUL (Fabrika Araç Lokasyonu): Araç Durum Kodu:
Üretim Tarihi: 26-May-2010 14:38:03 Sevkiyat Tarihi: 26-May-2010 16:12:01 Sevkiyat Tarihi: 26-May-2010 16:29:53
Sevk Durumu: (Sistem Hesabı: Sevkedilebilir)
Problemler Açık: 0 Problemler Kapalı: 0 Problemleri Toplamı: 0
Filo Sayımı: 0 İyi: 0 Kötü: 0 Suspect: 0
Bilinen Nakledilen/Yayınlanmış Araçlar: Evet
PUL tarafından öne sürülen nakil zorunlulukları: CHECKPOINT-CONNECT

rincil Lokasyon	Zaman-Değeri	Araç Problemi	Değerlendirme Yorumu	Çizim İsmi	Ad	Zaman-Değeri	Sebep Olan Pa
ı ARKA TABAN	25-May-2010 09:38:49:99						
ı ANA TABAN	25-May-2010 12:50:09:58						

Figure 3.4 : An example of process control report.

Also for torque measurement are taken from vehicles for eliminating bolt torque value variation. Torque measurement results on vehicles with after mileage has been started. Results of running vehicles are appropriate to the specifications. For 22.370 km mileage vehicle results please see Table 3.1.

Table 3.1 : RR Bracket Torque Measurements of Vehicle 9D29656 (22370km)

Application	Type	Check value	Minimal	Nominal	Maximum	Visual check
RR Bracket on Transmission	M10 x 35 Screw	52.8	38.43	47.5	62.76	OK
RR Bracket on Transmission	M10 x 35 Screw	47.7	38.43	47.5	62.76	OK
RR Bracket on Transmission	M10 x 35 Screw	45.5	38.43	47.5	62.76	OK
RR to Subframe	M10 x 70 Bolt	43.5	43.43	50	68.76	OK
RR to RR Bracket	M10 x 80 Bolt	43.6	43.43	50	68.76	OK

For torque measurements after 8 km – Squeak & Rattle Track running vehicle results please see Table 3.2.

Table 3.2 : RR Bracket Torque Measurements of Vehicle 9D29656 (8km – Squeak & Rattle Track additionally)

Application	Type	Check value	Minimal	Nominal	Maximum	Visual check
RR Bracket on Transmission	M10 x 35 Screw	42.8	38.43	47.5	62.76	OK
RR Bracket on Transmission	M10 x 35 Screw	44.8	38.43	47.5	62.76	OK
RR Bracket on Transmission	M10 x 35 Screw	50.7	38.43	47.5	62.76	OK
RR to Subframe	M10 x 70 Bolt	50.2	43.43	50	68.76	OK
RR to RR Bracket	M10 x 80 Bolt	50.2	43.43	50	68.76	OK

In addition to torque measurement from vehicles with after mileage, 50 audit torque measurements had been requested from assembly shop to see capability of assembly shop torque-process. When measurement results of 3 connections (RR bracket to

Transmission) are analysed in Minitab using the Weibull distribution, the output in Figure 3.5, Figure 3.6, and Figure 3.7 are generated.

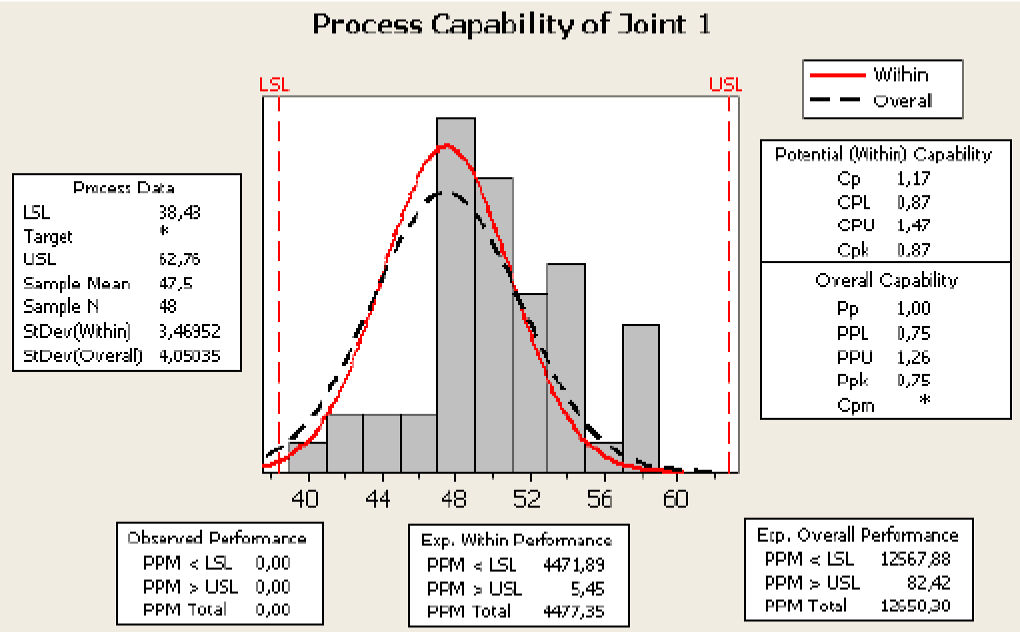

Figure 3.5 : Process Capability of Joint 1.

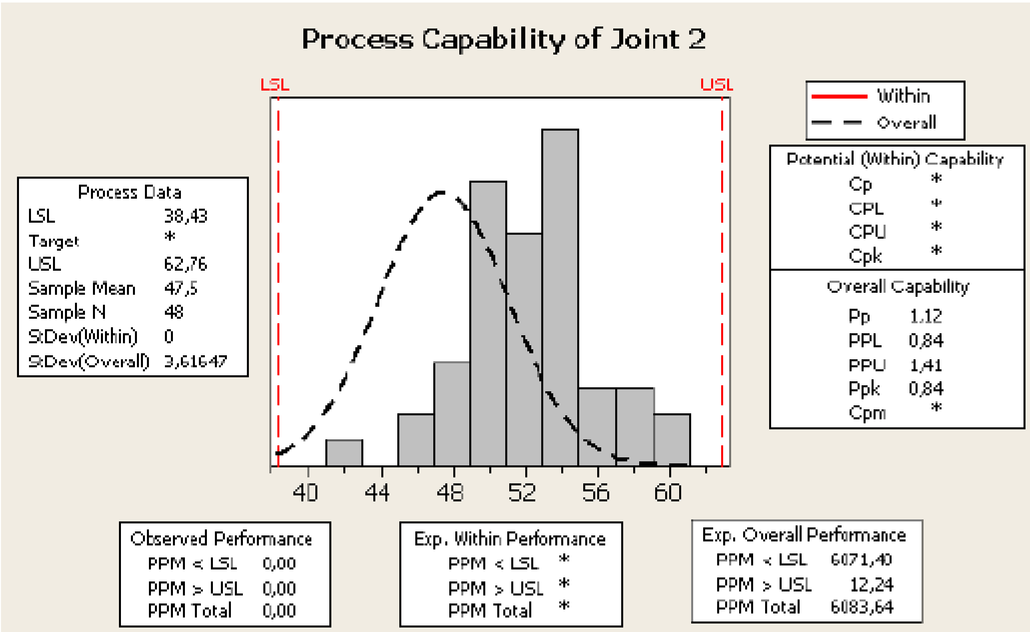

Figure 3.6 : Process Capability of Joint 2.

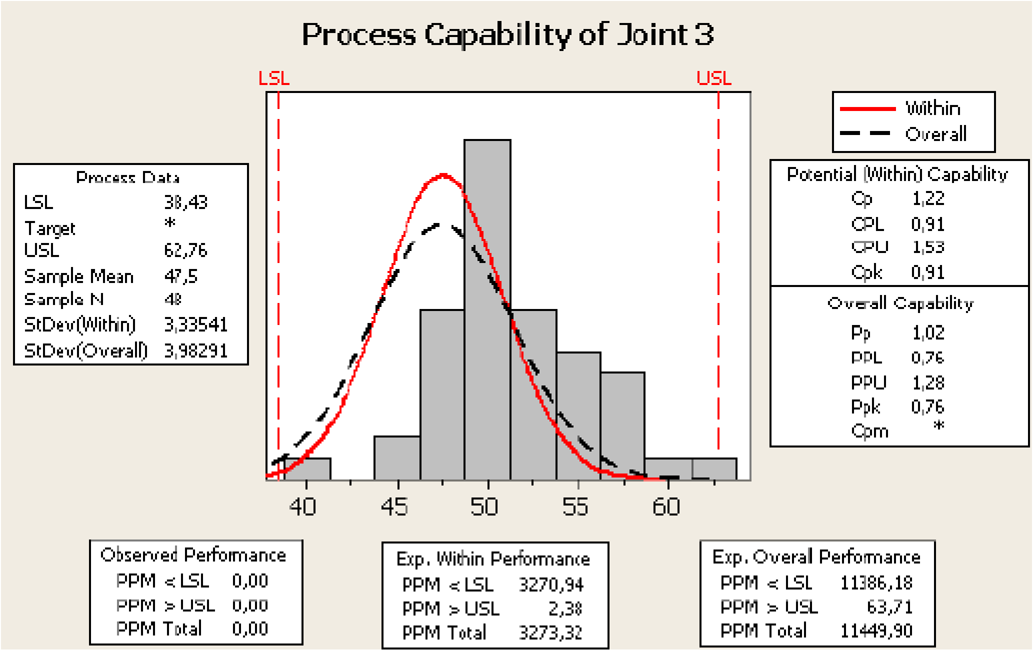

Figure 3.7 : Process Capability of Joint 3.

Figure 3.5, Figure 3.6, Figure 3.7 contains the Weibull plot for the observed results that there is no part out of specification. However, Weibull plot predicts that 4477,35(a) and 3273.32 (c) parts per million will not be in specifications if process is continued in this manner. According to the assembly shop records, Weilbull plot prediction can be ignored for this process.

3.2.2 Production line process

High impact-load failure can be also caused by worse production process that can cause to porosity, and some defects on part. For optimization of cost and robustness issue, both alternative supplier and current production supplier are studied. However, when the current supplier tool is inspected, some defects are seen such as porosity (Figure 3.8), due to almost completion of expected life of the mould and lack of sequence in porosity inspection. This means current supplier should change the production tool and increase the sequence of porosity inspection.

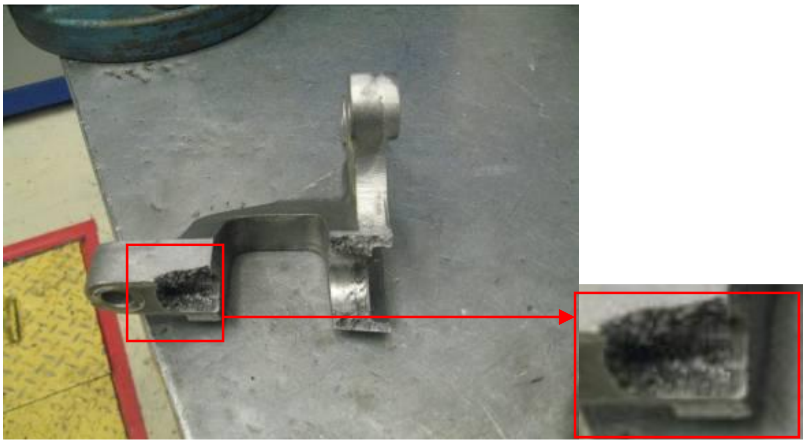

Figure 3.8 : Current supplier bracket brakeage due to the porosity issue.

For the alternative supplier, production tool was new, and certification to serial production was taken. However, a failure was seen in impact testing that will be discussed next chapter. To eliminate porosity effect, analyses were done with proper tool. Results are seen in Figure 3.9 to Figure 3.14.

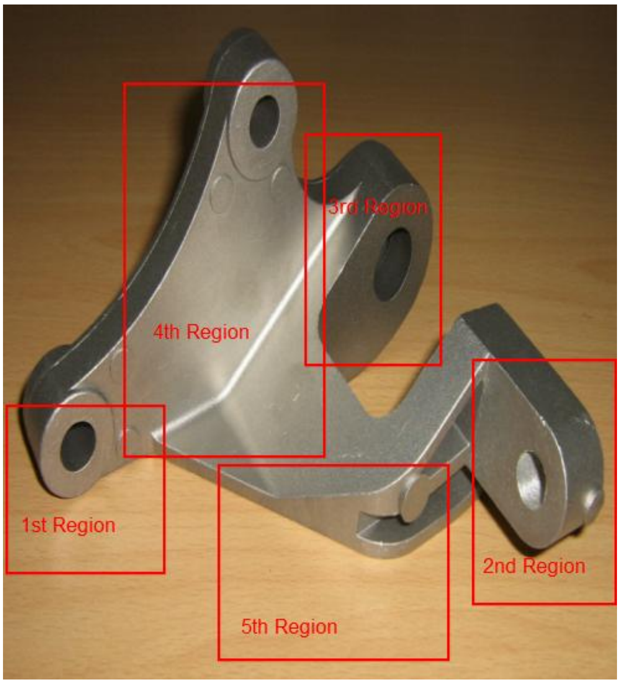

Figure 3.9 : Porosity analyses locations.

The porosity inspection of the 1^{st} region as seen in Figure 3.10 was done with 61.0 kW--1.-90 mA. It is in Level 1 according to ASTM E 505 Standard.

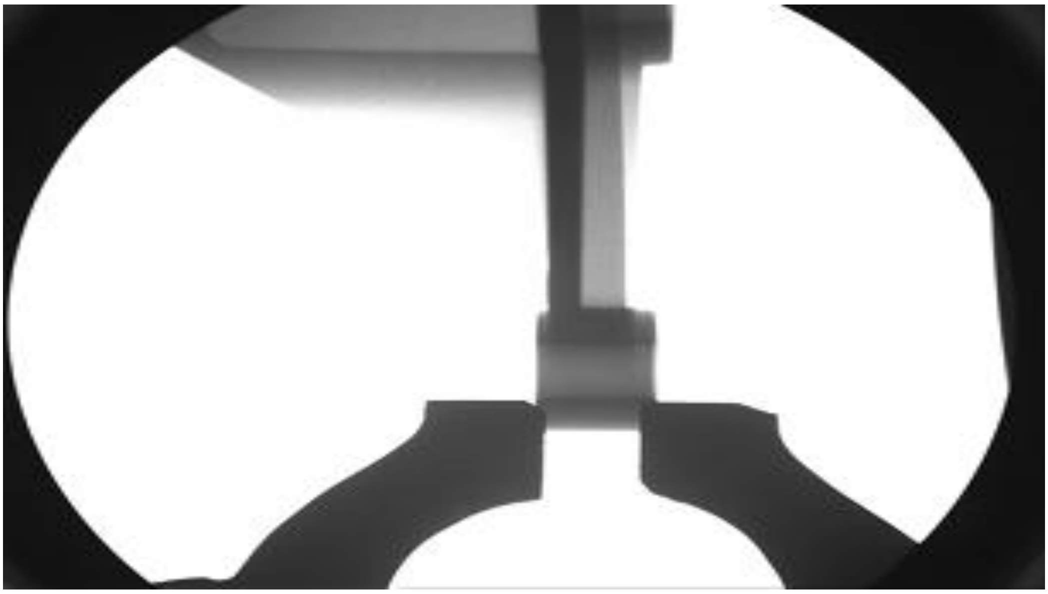

Figure 3.10 : Porosity inspection for the 1st region.

The porosity inspection of the 2nd region as seen in Figure 3.11 was done with 63.0 kW--2.00 mA. It is in Level 2 according to ASTM E 505 Standard.

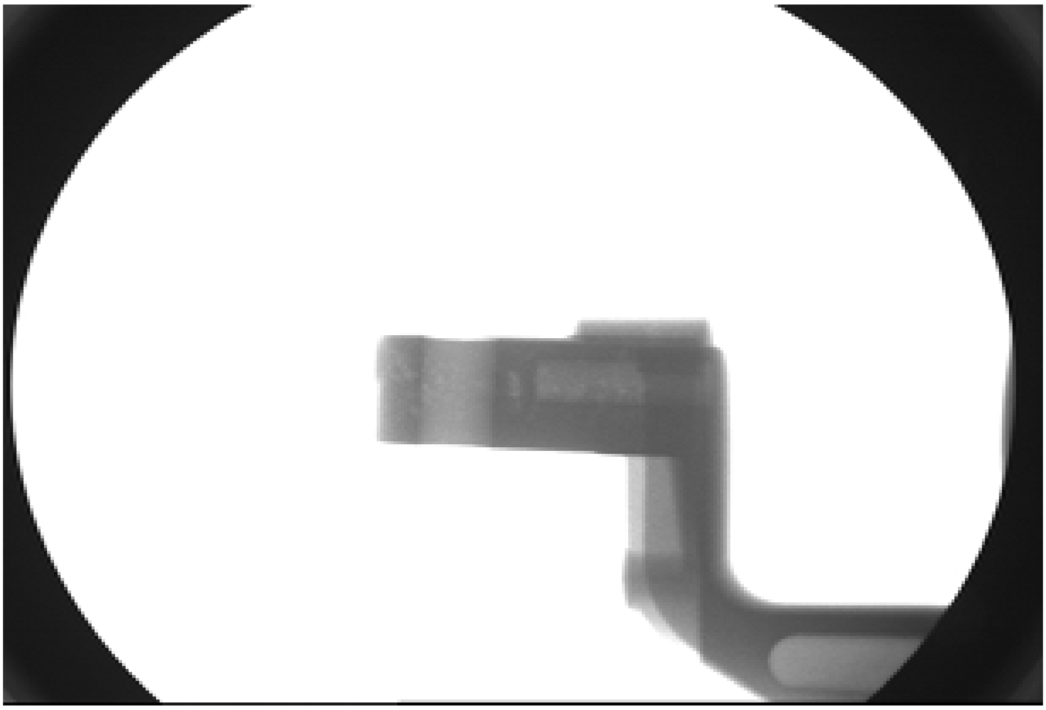

Figure 3.11 : Porosity inspection for the 2nd region.

The porosity inspection of the 3rd region as seen in Figure 3.12 was done with 66.0 kW--2.10 mA. It is in Level 1 according to ASTM E 505 Standard.

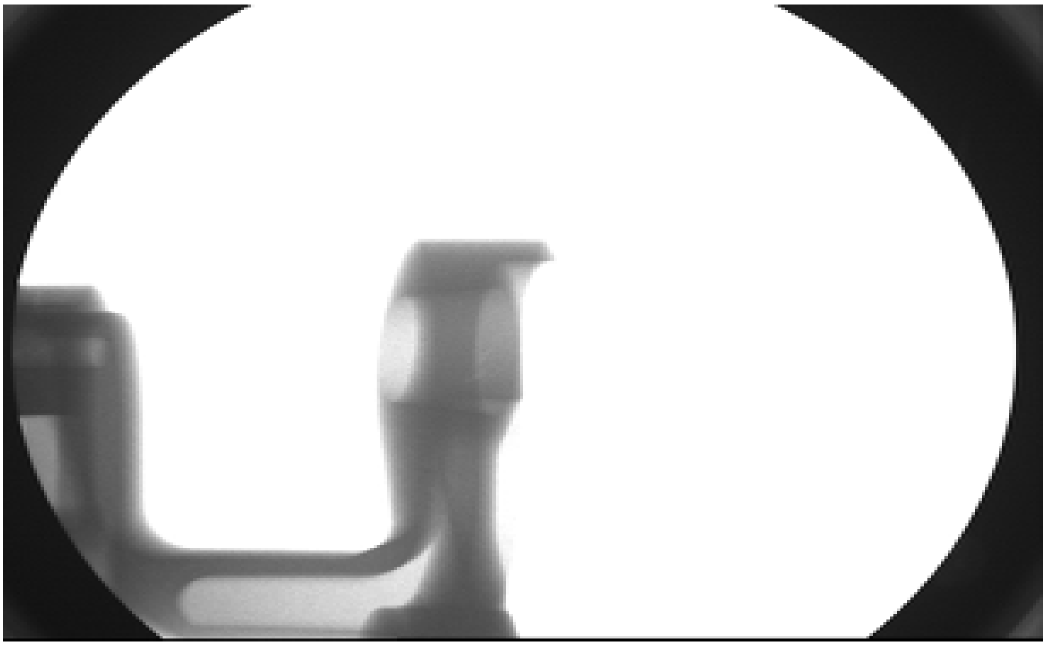

Figure 3.12 : Porosity inspection for the 3rd region.

The porosity inspection of 4th region as seen in Figure 3.13 was done with 58.0 kW--1.70 mA. It is in Level 1 according to ASTM E 505 Standard.

Figure 3.13 : Porosity inspection for the 4th region.

The porosity inspection of 5th region as seen in Figure 3.14 was done with 62.0 kW--2.10 mA. It is in Level 1 according to ASTM E 505 Standard.

Figure 3.14 : Porosity inspection for the 5th region.

All results for all locations are Level 1 and Level 2 where the accepted value is Level 3 and better (1-3) referring to ASTM E 505. This porosity specification is taken from Ford TRR Bracket Engineering Specification (2004).

In addition, alternative supplier has applied finer surface finish as an improvement that affects the long-life fatigue (Juvinall and Marshek, 1991).

3.2.3 Material properties

For TRR bracket, material is stated as EN 1706 group aluminium alloys. The current supplier has selected EN 46200 AlSi8Cu3 (Fe) and the alternative supplier has selected EN 46000 AlSi9Cu3 (Fe). These two aluminium alloy belongs to same group and their tensile, elongation and mechanical properties almost same with each other. To eliminate the effects of material properties, chemical composition, and hardness analysis have done for each supplier.

Material and hardness specifications are taken from British Standard EN 1706:1998 and all harness and material composites are in specifications for both suppliers (for test results please see Appendix B). For both high-pressure aluminium alloys' mechanical properties are shown in table.

Table 3.3 : EN 46000 and EN 46200 group pressure die cast aluminium alloys mechanical properties

Material	Tensile strength MPa min.	Proof stress MPa min.	Elongation % min.	Brinell hardness HBS min.
EN 46200 AlSi8Cu3	240	140	1	80
EN 46000 AlSi9Cu3(Fe)	240	140	<1	80

For the chemical composition of the AlSi9Cu3 (Fe) and AlSi8Cu3 table is also taken from British Standard EN 1706:1998 (for BS EN 1706:1988 tables please see Appendix A) .

Table 3.4 : Chemical composition of Aluminium casting alloys EN 46000 and EN 46200 in % by mass

Material	Si	Fe	Cu	Mn	Mg	Cr	Ni	Zn	Pb	Sn	Ti
EN 46200 AlSi8Cu3	7,50-9,50	max. 0,80	2,00-3,50	0,15-0,65	0,05-0,55	-	max. 0,35	max. 1,20	max. 0,25	max. 0,15	max. 0,25
EN 46000 AlSi9Cu3(Fe)	8,00-11,00	max. 1,30	2,00-4,00	max. 0,55	0,05-0,55	max. 0,15	max. 0,55	max. 1,20	max. 0,35	max. 0,25	max. 0,25

3.2.4 Design parameters

As seen in warranty data most of the failure mode has occurred in low mileage that was indicated that failures occur due to the high impact loads in the beginning of the Section 3.1. Customer misusage may cause such impact-loads. These abused loads are higher than standard customer usage in worst case condition and to eliminate this effect, special component and vehicle level tests were done in cycle base that will be reviewed in Chapter 4. Before going to change in design, current and alternative supplier's brackets should be tested for comparison of tooling and surface finish terms.

4. INITIAL EXPERIMENTAL STUDIES

For the experimental studies Ford design verification checklist was reviewed that includes testing to be done that represent worst-case real life conditions. As in the checklist, vehicle level durability test for typical usage, driveline impact test for misusage, component level abuse and static tensile tests were done.

4.1 Vehicle Level Durability Test

The purpose of this test is to validate the strength, durability and functionality of all components of the vehicle over 240,000 km or 1 life - drive train, components of all types of light trucks, including, but not limited to rear axle, drive shaft (prop shaft), gearbox, clutch and engine mount system. Vehicle durability test includes typical driving condition and misusage is not included. All components that complete this test without failure are considered to be durable. For a good evaluation, it is mandatory that this procedure is executed as accurately as possible.

Only alternative supplier's prototype was sent to Lommel Proving Ground as current production part has already sign-off with durability test. Tested part photographs are shown in Figure 4.1.

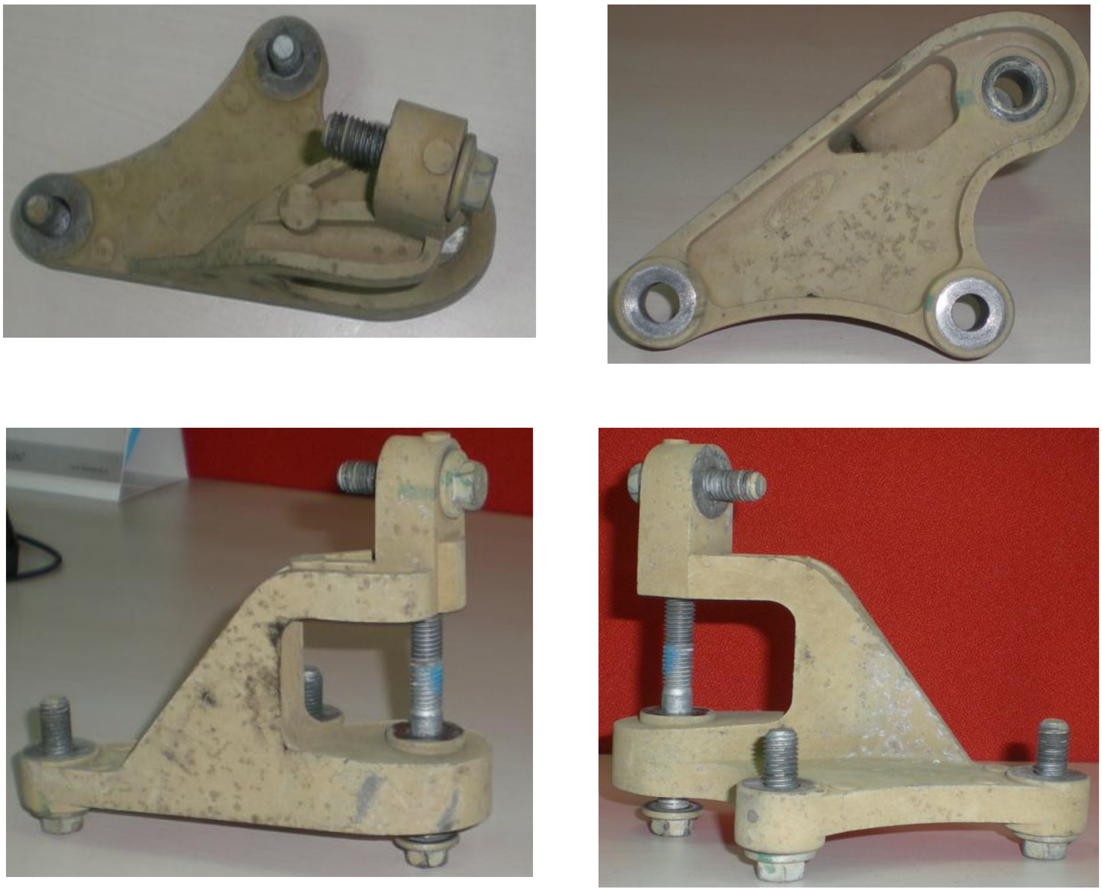

Figure 4.1 : Alternative supplier's TRR bracket prototype after vehicle level durability test, in different view.

4.2 Driveline Impact & Snap Start Test

The purpose of this test is to determine the durability and proper functioning of passenger car and light truck driveline components in the case of abrupt clutch engagement.

For FWD vehicles the Driveline Impact Test was performed a total of 90 impacts in the sequence below:

- Driveline Impact Forward Starts in 1st gear: Conduct a specified number of forward starts in 1st gear; while vehicle in rest, released brakes, 1st gear selected, and clutch disengaged. Accelerate engine to specified rpm, slip foot sideways from clutch pedal, keep throttle-pedal in constant position after engaging clutch, drive an "8" figure (to bring diff-gears to a new position).

- Driveline Impact Forward Stops in 1st gear: Conduct a specified number of stops in 1st gear; Accelerate vehicle in first gear up to specified rpm, disengage clutch and let vehicle roll until engine speed is down to specified rpm, slip foot sideways from clutch pedal, drive an "8" figure (to bring diff. – gears to a new position).
- Conduct a specified number of Driveline Impact Forward Starts in 1st gear
- Conduct a specified number of Driveline Impact Forward Stops in 1st gear
- Conduct a specified number of Impact Forward Starts in 1st gear
- Conduct a specified number of Impact Forward Stops in 1st gear
- Driveline Impact Test (reverse): Conduct a specified number of Driveline Impact Reverse Starts; while vehicle in rest, released brakes, reverse gear selected and clutch disengaged, accelerate engine to determined rpm, slip foot sideways from clutch pedal, keep throttle-pedal in constant position after engaging clutch (sandbag under pedal), drive an "8" figure (to bring diff.-gears to a new position).
- Conduct a specified number of Driveline Impact Reverse Stops; accelerate vehicle in rev. gear speed up to determined rpm engine speed, disengage clutch and let vehicle roll until engine speed is down to determined rpm, slip foot sideways from clutch pedal, drive an "8" figure (to bring diff.-gears to a new position).
- Snap Starts: Conduct a specified number of starts in low as follows; Vehicle stationary, released brakes, 1st gear selected, and clutch disengaged, Rev up and hold engine speed at determined rpm, slip foot sideways from clutch pedal, WOT immediately after clutch engagement until achieving determined km/h, Drive an "8" figure (to bring diff.-gears to a new position).

Test was done for alternative supplier prototype part sign-off with 110PS A/C short wheel base vehicle with 90-cycle test. As a result cracked was occurred at 64^{th} cycle (in %71 of testing). For the failure location, please look at Figure 4.2.

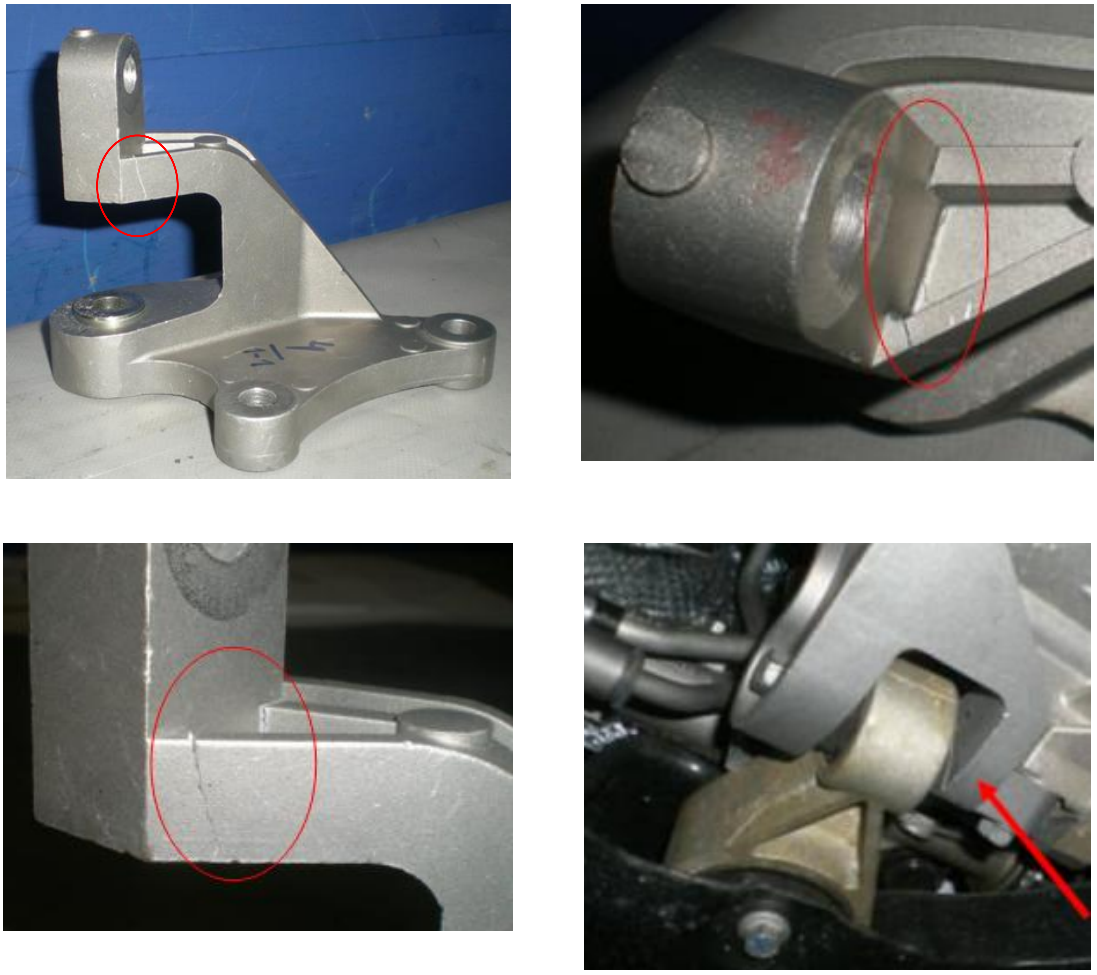

Figure 4.2 : Alternative supplier's TRR bracket prototype after Driveline Impact and Snap Start Test, in different views.

4.3 Static Tensile Test

With respect to tensile durability of TRR bracket, a series of static tensile tests were performed on the Instron piston in Gölcük Plant Test Centre (Figure 4.3). These tests would provide a comparison of the performances of the bracket designs in terms of tensile loading. The expected minimum load to failure is 50 kN that comes from roll restrictor mount aluminium side design verification plan.

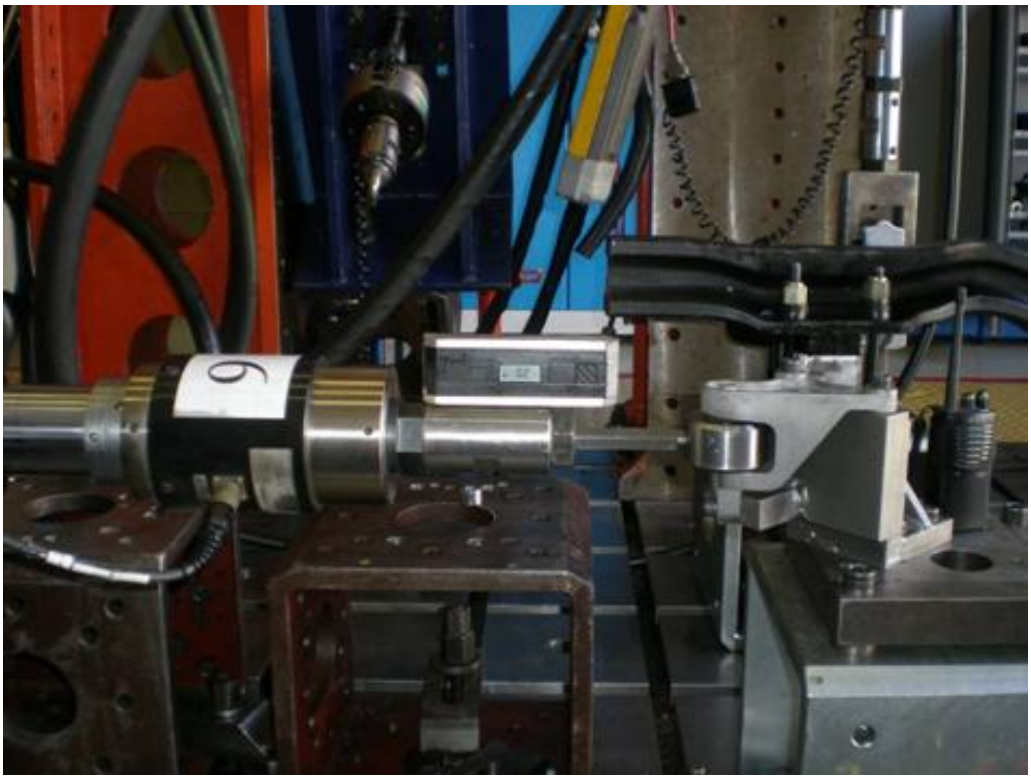

Figure 4.3 : Static tensile test rig.

For the static tensile test rig and the failed parts please see Figure 4.4:

Figure 4.4 : Failed parts in static tensile test.

Table 4.1 : Static tensile test results for all production and prototype parts

Supplier	Level	Failure Load	Status
Alternative	Old	43.11 kN	Failed
Alternative	Old	39.69 kN	Failed
Alternative	Old	41.99 kN	Failed
Alternative	Old	45.28 kN	Failed
Current	Old	25.76 kN	Failed
Current	Old	37.49 kN	Failed
Current	Old	31.86 kN	Failed
Current	Old	31.84 kN	Failed

Results show that both current and alternative supplier failed from static tensile test. However, current supplier production tool and coarse surface finish affect the results in a bad way.

4.4 X-Direction Abuse Test

FoE generates a low cycle fatigue load to be applied 100 times positive and negative in vehicle x, 1000 times in y and z (for roll restrictor bracket only x-axis is determining factor). This load is used for metal testing (CAE and rig). In the x-direction, this is scaled from Ford Focus data collected from abusive wheel stick-slip and clutch side-step events to represent the worst-case powertrain induced loads. There are three vehicle durability-test-cycles, all essentially customer correlated for 95th percentile customers of cars, vans and light trucks.

The P/T Mount Abuse and Peak Durability (100 & 1000 cycle) load cases are simple single axis sinusoidal tests which are utilised to design and prove out the strength and durability of metallic components. Loads levels are calculated using simple scaling equations based on torque & mass. These events should exceed the damage from any measured data by a sufficient margin to account for vehicle to vehicle variability and ideally negate the need for any multi-axial load cases.

Abuse load (100 cycles) generated from an extreme event not usually part of normal driving. Typically it relates to high torque in combination with intermittent wheel slip.

The magnitude of this load case should be defined so that it is no lower than that found when considering the following events from similar powertrains and mount architectures on the same platform:

- The peak load from the combined driveline impact and stop start test
- The peak load from the entire durability route.
- The equivalent load @ 100 cycles from a fatigue reduction of the entire durability route
- Special events (where appropriate, e.g. off road vehicle ditch drop)

To determine whether both suppliers' TRR bracket would perform adequately, a series of tests were performed on the Instron cyclic test rig in Gölcük Plant Test centre. These tests would provide a comparison of the performances of the bracket designs in terms of low cycle fatigue under high impact load.

Four bracket were taken randomly from the assembly production line (as current supplier production), and four prototype bracket were taken from alternative supplier. Standard production bracket bolts were used to retain the bracket. All are torqued to 47.5 Nm. Each bracket was then mounted on the Instron piston with a special arm simulating roll restrictor, and subjected to a cyclic loading of ±28kN with specified frequency. The tests were suspended at 200 cycles if no failure occurred.

Alternative and current supplier's test results are shown in Table 4.2.

Table 4.2 : X-direction abuse test first results for alternative supplier

Supplier	Level	Failure cycle	Status
Alternative	Old	60 cycle	Failed
Alternative	Old	65 cycle	Failed
Alternative	Old	33 cycle	Failed
Alternative	Old	82 cycle	Failed
Current	Old	32 cycle	Failed
Current	Old	4 cycle	Failed
Current	Old	8 cycle	Failed
Current	Old	2 cycle	Failed

One can also see the critical points of failure from the photographs as shown in Figure 4.5 and Figure 4.6.

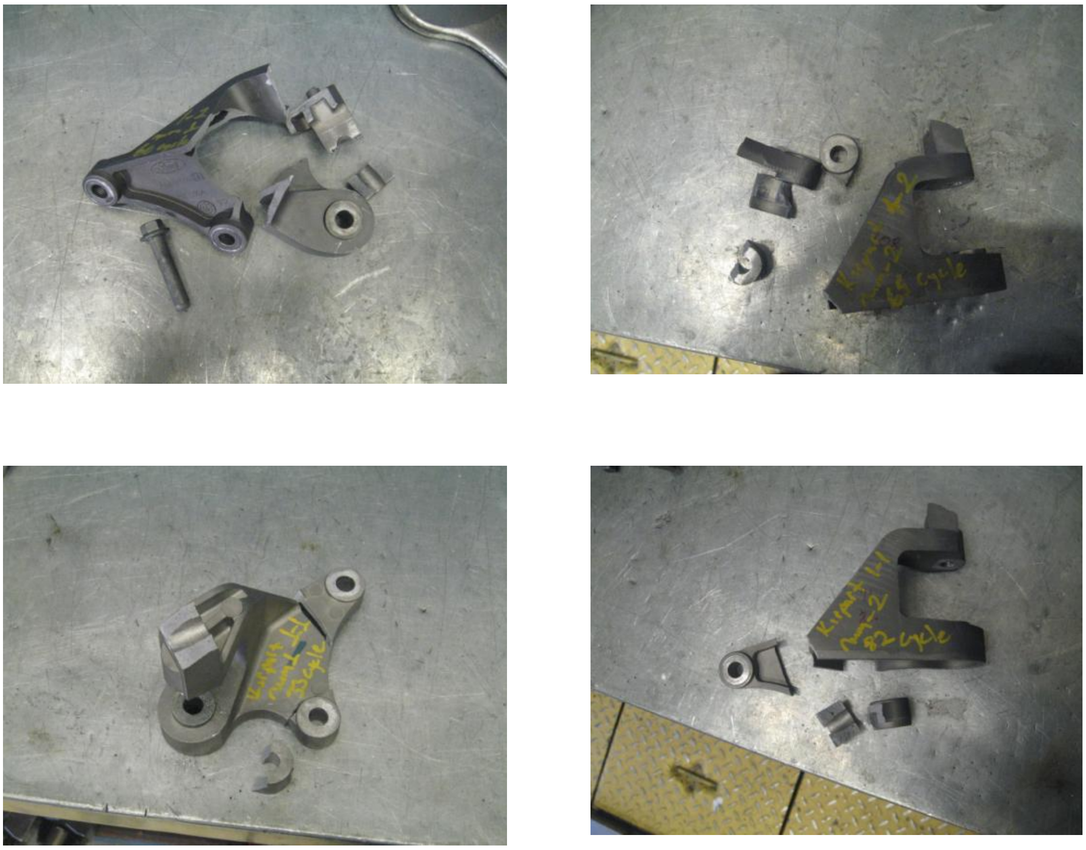

Figure 4.5 : Alternative supplier's prototypes photographs taken after x direction abuse test.

Figure 4.6 : Current supplier's prototypes photographs taken after x direction abuse test.

As summary, the expected minimum life of a TRR bracket at this loading is 100 cycles. All of the brackets failed before expected minimum life. The common failure locations are displaced in red circles. As seen on the photographs referred locations are the common and most critical points with respect to low cycle reversal fatigue loads.

4.5 Discussion of Initial Testing Results

As a result of comparison of two suppliers, alternative supplier production process capability in terms of porosity and surface finish quality provide better static tensile durability (Figure 4.7) and abuse load durability results (Figure 4.8).

However, durability improvement is provided with process improvement, it is not enough to provide Ford TRR Bracket Engineering Specification (2004) of the bracket by own. For the improvement of the durability life cycle, design should be improved in terms of geometry, additionally.

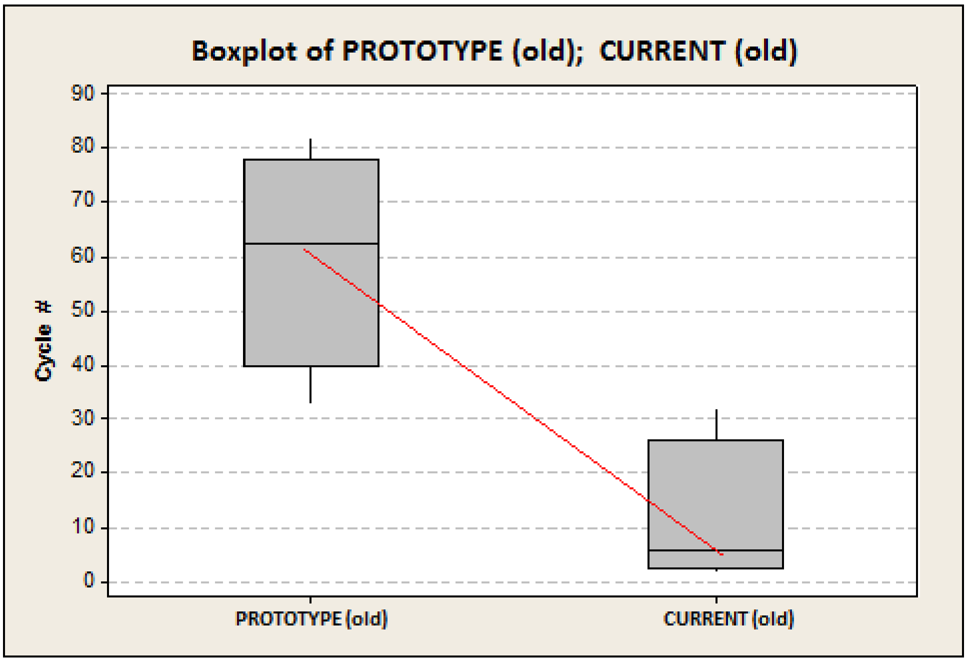

Figure 4.7 : Abuse load durability comparison of alternative supplier vs. current supplier.

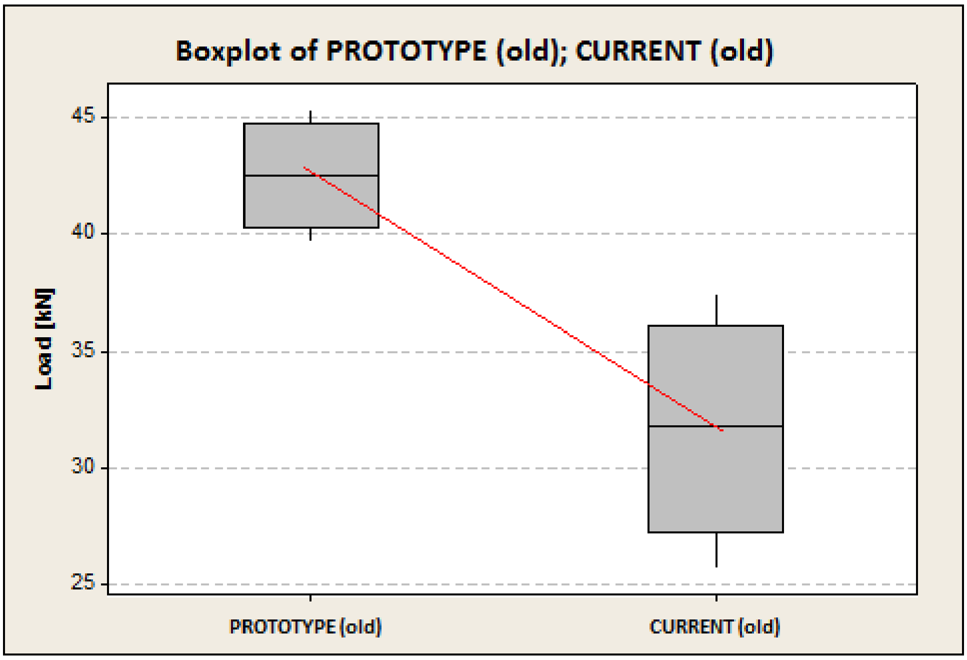

Figure 4.8 : Abuse load durability comparison of alternative supplier vs. current supplier.

From this point forward, alternative supplier's prototype will be taken as reference in terms of material properties and testing samples.

5. FINITE ELEMENT ANALYSIS OF THE TORQUE ROLL RESTRICTOR BRACKET

As mentioned by Wilson (2004), once the loads are known then they can be applied on bracket and the software predicts the stresses and strains around the part. These results are then analysed to determine whether the part meets the required durability requirements at this stage. As has been mentioned, this is a crucial area of the modern development process; both in terms of piece cost and development time reduction.

Although employing different software packages, the different brands use fundamentally similar software techniques to model their components. Ford of Europe Team analyses parts using a combination of IDEAS and NASTRAN modelling. For Aluminium parts, Ford only uses Linear NASTRAN analysis (although the Tier 1 suppliers to Ford of Europe use non-linear methods to deal with the elastomeric parts and Ford uses ABAQUS for steel components). Both Volvo and Land Rover use NASTRAN for Modal/Mobility analysis of the parts and ABAQUS for Non-Linear stress analysis (contact analysis, bolt pre-load and friction). Land Rover also uses MASTER SERIES for Linear analysis and Modal/Mobility analysis. For Otosan also uses OPTISTRUCT for Engine Support Brackets.

The Ford of Europe Powertrain Mounts team has their own CAE guideline (Farrington et al., 2003). These outline the process to be followed by the suppliers to ensure consistent results are achieved. The guidelines start by setting out the responsibilities of the supplier and the Ford team in the development and sign off of the CAE of the parts (which occurs before tooling the parts). The document gives some general guidance on modelling in addition to specific guidelines on mesh quality to be used, representation of bolted joints, constraints and boundary conditions, checks that should be performed both before and after analysis along with some specific lessons learned from previous issues. In addition, stress factors are covered in guideline to take account of non-reversible stress, non-homogeneity and surface finish, geometry variation and FEM quality. In Chapter 2, as the background of the study, stress factors and formulations are covered. The CAE guidelines are intended to be used in tandem with the P/T Mounts Design Review (2004), which run through the durability testing process for component tests. This section covers the modelling of aluminium TRR bracket with steel insert and checking of the FEM. At the end of the chapter the FEA stress results will be discussed by comparison to testing results in durability-life base.

Figure 5.1 illustrates the V227 torque roll restrictor assembly. The piece to the left of the Figure 5.1 is the roll restrictor; a pressed steel housing, into which the large rubber bush is fitted. On both of the large and the small rubber bush has a steel ring around it and has a high pressure die cast aluminium core. On the right of the Figure 5.1 is the transmission bracket. This is a high-pressure die cast aluminium bracket with a small steel insert fitted into it (where the roll restrictor is bolted to it).

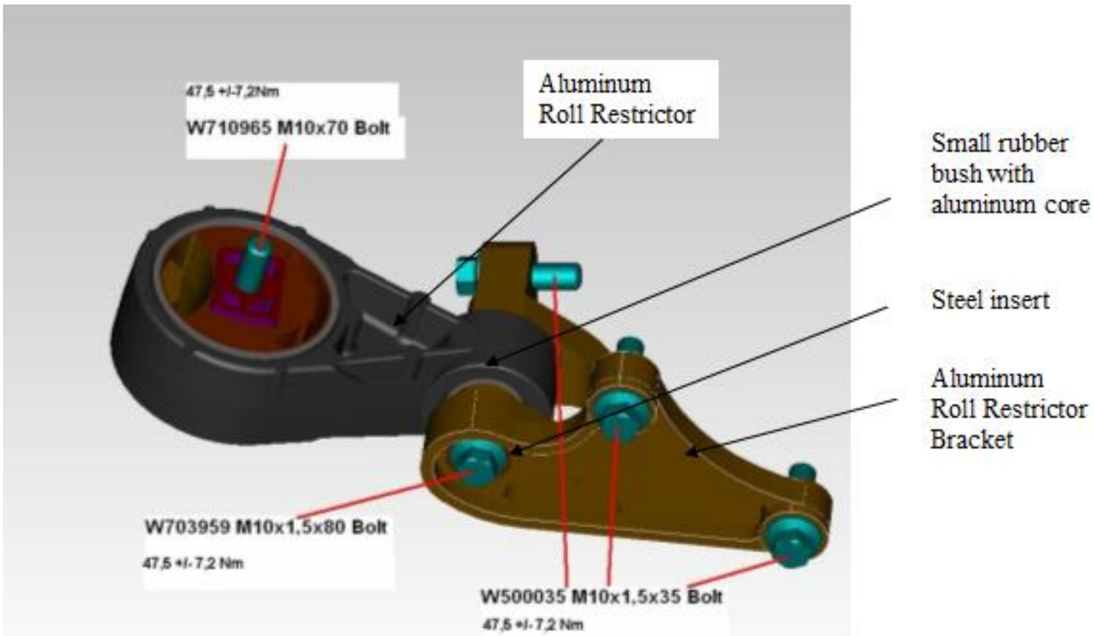

Figure 5.1 : Roll Restrictor Mount and Bracket Assembly.

5.1 Finite Element Model of TRR Bracket

Finite element model is built up with respect to Modelling, Analysis and Reporting Guidelines (Farrington et al., 2003). First of all 2D tria mesh is used for aluminium shell with 0.01mm thickness to see surface stresses, and to complete 3D tetra mesh to create solid model.

The bracket geometry and the critical points were considered while choosing 2D mesh element size. Firstly, there should be at least two meshing elements in a line of geometry width or height for healthy results. Secondly, on the critical points, stress levels will not be changed by greater than 10 percent with using finer mesh size. Finally, mesh size should be in optimum size to get the healthy results in a short time. For this model 3mm mesh size was chosen as general and 1.5 mm mesh size was chosen for critical points.

Before create tetra meshes quality index of trias, connectivity and duplicates were checked in terms of aspect ratio, minimum and maximum of tria angles (Figure 5.2).

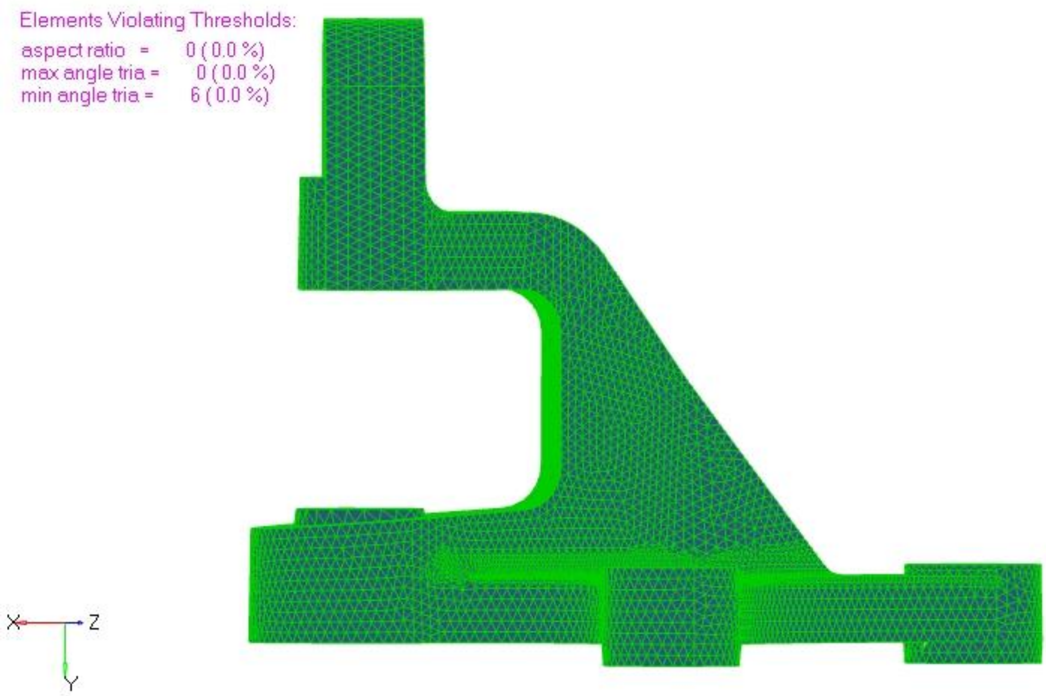

Figure 5.2 : Element violating threshold values.

After all 2D meshes are checked 3D tetra meshes were created with 2nd order. Tetra collapse was checked for element quality as seen on Figure 5.3 and Figure 5.4.

While creating steel bush and aluminium bracket, they were considered as belonging to one solid part. There was no surface element between steel and aluminium fitting faces.

Before building base model, steel insert was modelled as selected tetra meshes under certain insert diameter and were moved into other component that created before. The properties were assigned to components in terms of their material. For the Aluminium bracket material properties were entered as 2.7e-6 g/mm3 as density, 70 GPa as Elastic modulus and 0.33 as poisons ratio. These values were 7.9e-6 g/mm3 as density, 210 GPa as Elastic modulus and 0.3 as poisons ratio, for the steel insert and bolts.

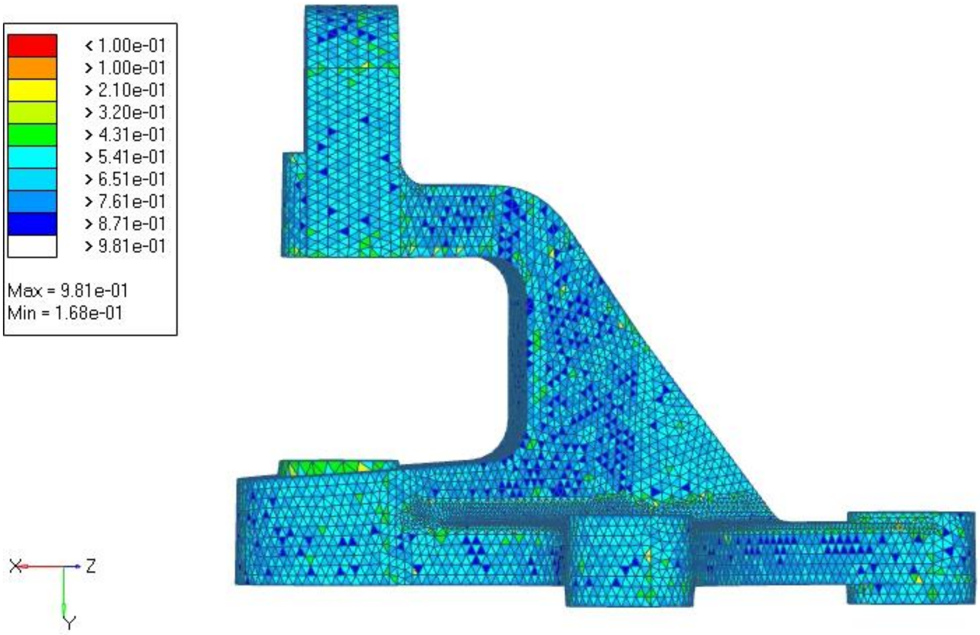

Figure 5.3 : Tetra collapse status from xy axes.

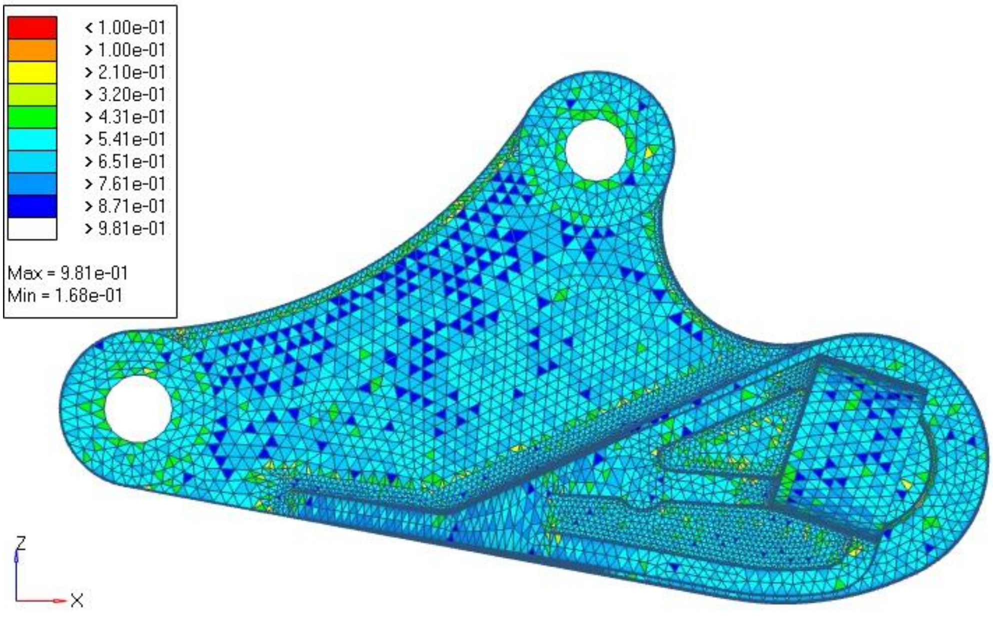

Figure 5.4 : Tetra collapse status from zx axes.

Base model was built with bars as bolt and screws, rigid as contact surfaces of brackets with bolt head and transmission, single point of contacts as boundary conditions and forces that directly applied to the bracket via bolts and roll restrictor (Figure 5.5, Figure 5.6, and Figure 5.7).

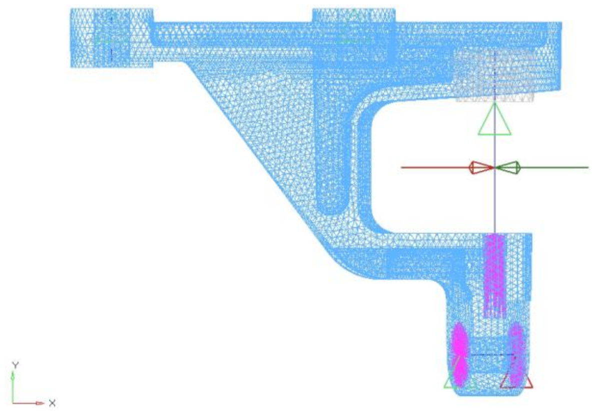

Figure 5.5 : Finite element model of roll restrictor bracket in yx view under positive (red coloured) and negative (green coloured) load conditions.

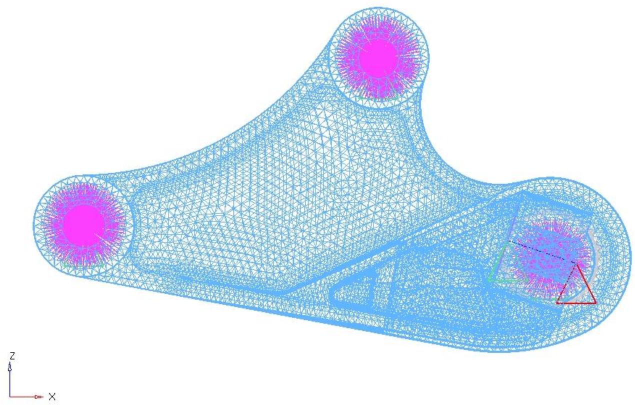

Figure 5.6 : Finite element model of roll restrictor bracket in zx view under positive (red coloured) and negative (green coloured) load conditions.

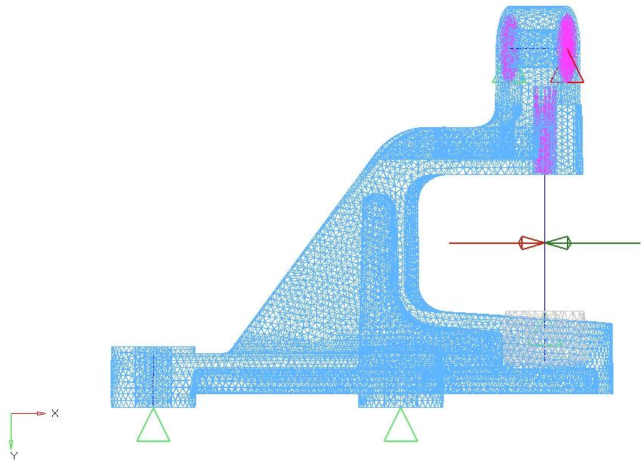

Figure 5.7 : Finite element model of roll restrictor bracket in xy view under positive (red coloured) and negative (green coloured) load conditions.

In this study, Altair HyperWorks OPTISTRUCT tool is used to analyse the aluminium TRR bracket. Control cards for the OPTISTRUCT linear static analyse model were completed in Hypermesh. Two load steps were defined for negative (green coloured) and positive (red coloured) direction loads. After control cards were defined, model was sent to NIC (Numerically Intensive Computing) via web to run the analysis.

5.2 First Results

After the result file was loaded, Von-misses stresses and displacement on the bracket were checked for confirmation of mechanism of the deformation. The critical location is seen shown in the Figure 5.7 and Figure 5.8.

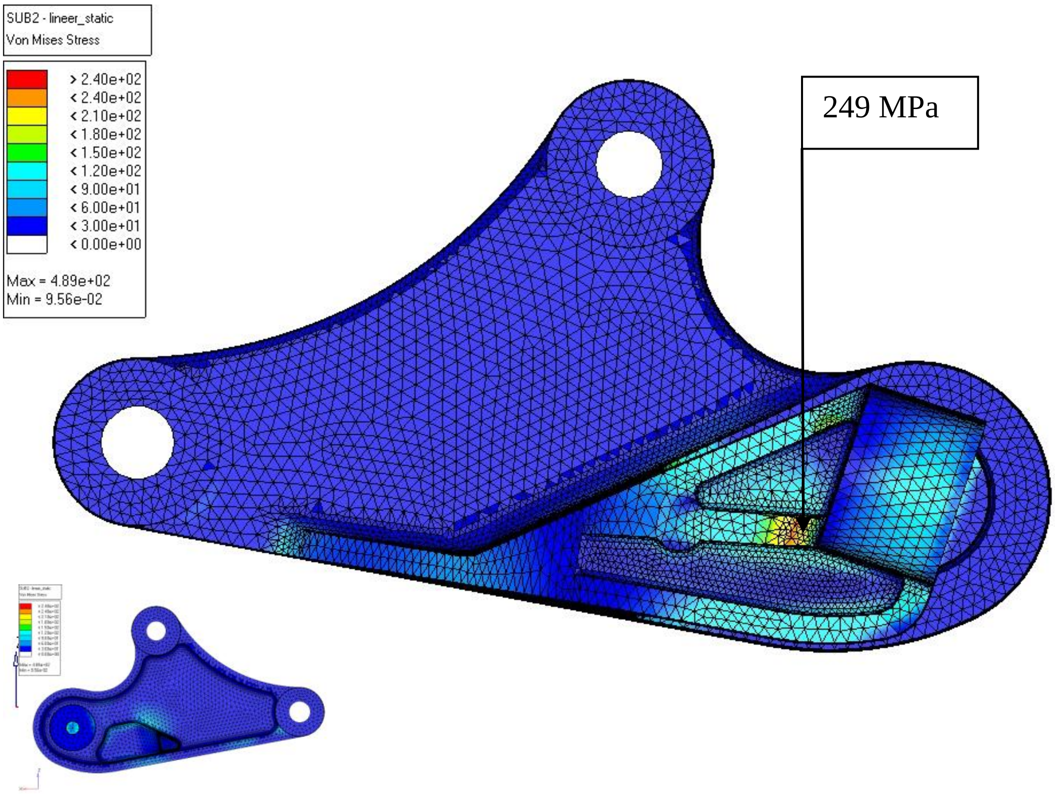

Figure 5.8 : Critical locations for the base design in positive linear loading.

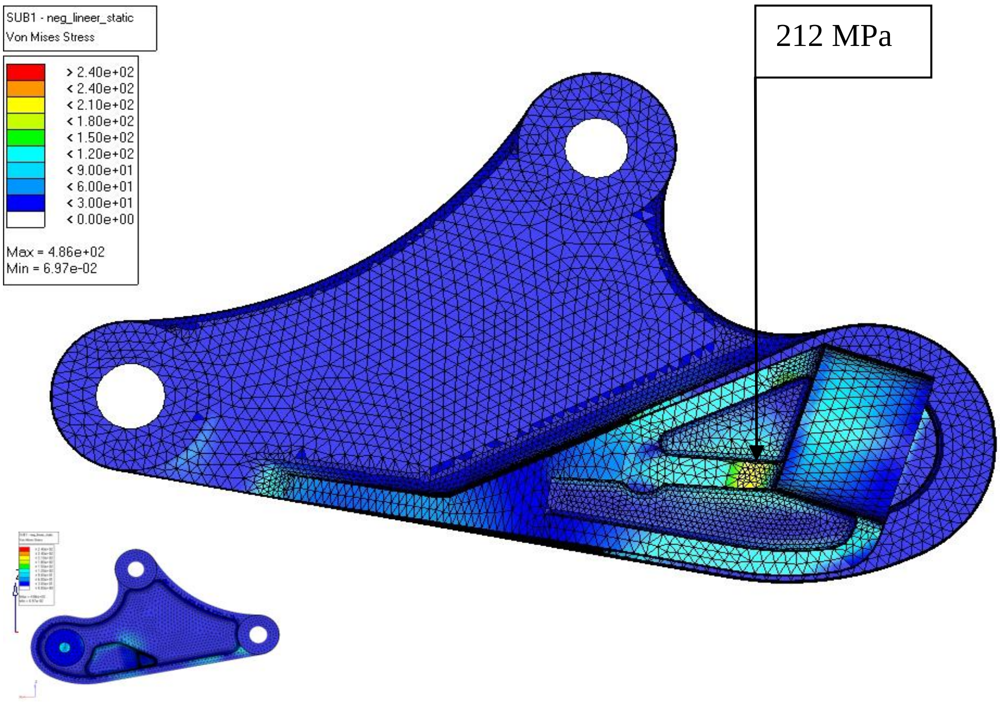

Figure 5.9 : Critical locations for the base design in negative linear loading.

Critical locations are same in both positive and negative linear static FE analysis results. The most critical locations are the turret radii that were also failure locations in Drive-Line Impact Test. Other two regions are less critical but there were failures seen in x-direction abuse test and static tensile test from that location (Figure 5.10).

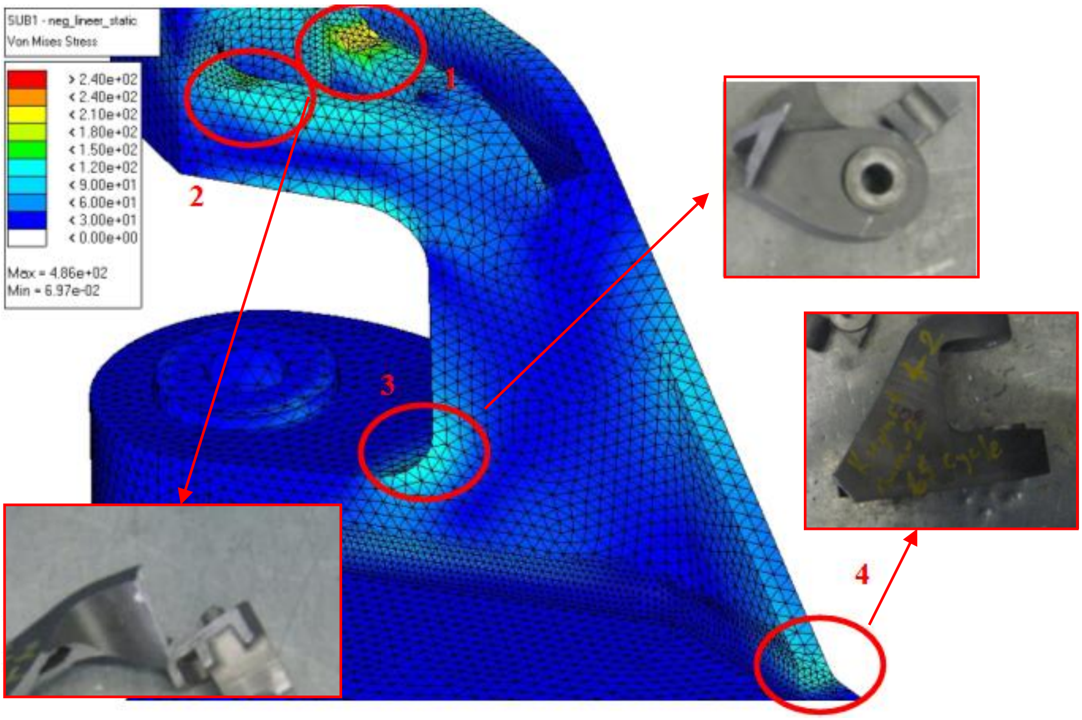

Figure 5.10 : Critical locations for the base design.

For the base design model, FEA results are documented in Table 5.1, as referenced to critical points shown in Figure 5.10.

Table 5.1 : Von Misses stress values for base design in critical locations as referred in Figure 5.10

Design	Location	Loading	Von Misses Stress [MPa]
Base	1	Positive	249
		Negative	212
	2	Positive	157
		Negative	142
	3	Positive	131
		Negative	117
	4	Positive	62
		Negative	83

With respect to the FEA, under positive and negative reversible loading, the critical points Von Misses stress values are almost same, and have opposite sign of pressure values. For instance, for the turret radii are under compression while applying positive x-direction force and under tensile while applying negative x-direction force. For the life estimation the most critical point and largest Von Misses Stresses were used as the worst case condition. In case of positive loading, region one Von Misses stress value was read as 249 MPa. The Von Misses stress value and 1st testing results in life cycle terms were located into the S/N curve (Figure 5.11). Violet coloured values are belonging to current supplier and the red ones belonging to alternative supplier. As seen in the Figure 5.7 current supplier testing values are more close to the bottom line of the curves interval.

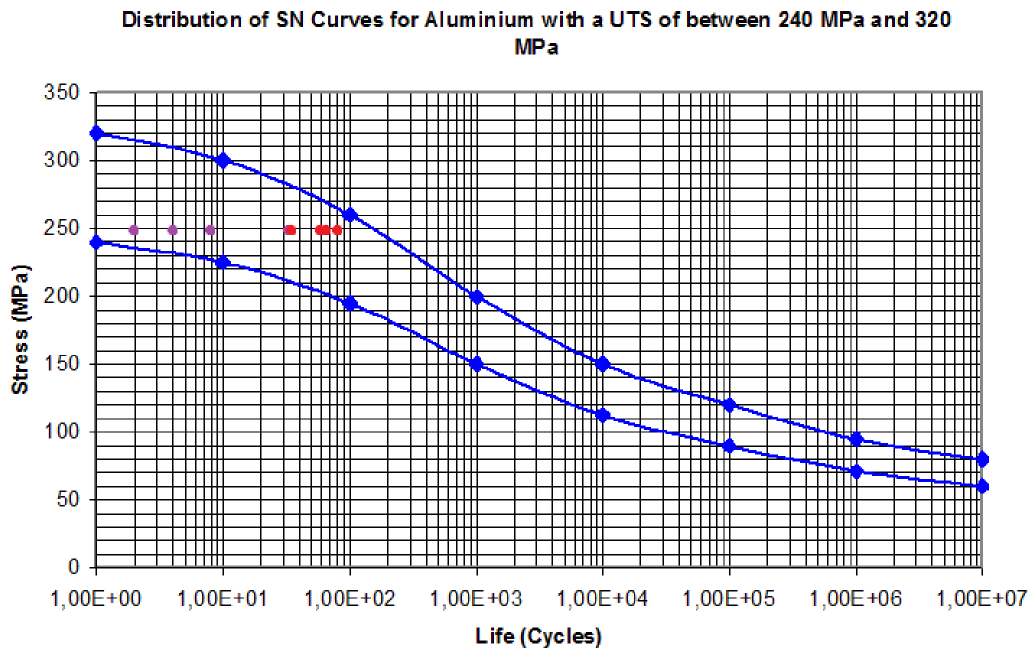

Figure 5.11 : First testing results and FEA stress results correlation on S/N curve for current supplier (violet coloured) and alternative supplier (red coloured).

As a result, all data seen are between curves and that refers to built FEM could be used in improvement study. After improvement takes place, all FEA results will be compared to testing results again and FEM model will be correlated totally with x-direction abuse testing.

5.3 TRR Bracket Design Improvement Study

To improve the critical locations' durability life, three alternative solutions were also analysed in Altair OPTISTRUCT. Alternative solutions were presented as gradually increasing radii or thickness of the ties in the critical locations (Figure 5.8). For the alternative solutions, same FEA procedures were followed, and same FEM was used.

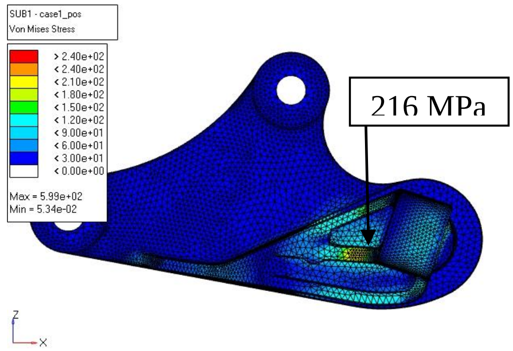

Figure 5.12 : Results of Option1 positive loading condition.

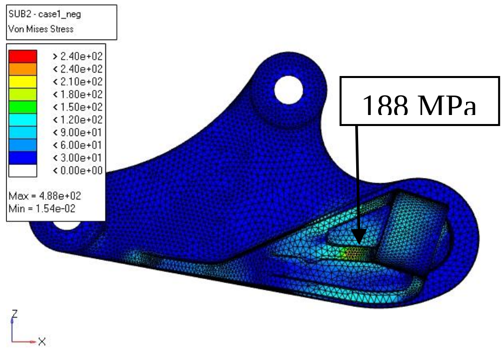

Figure 5.13 : Results of Option1 negative loading condition.

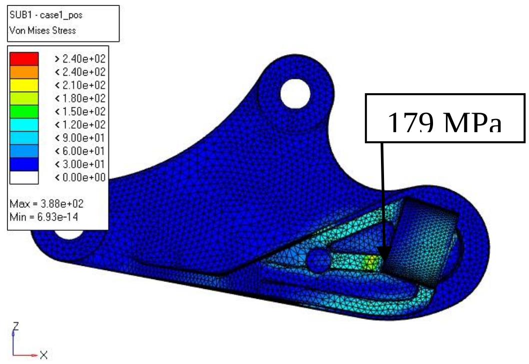

Figure 5.14 : Results of Option2 positive loading condition.

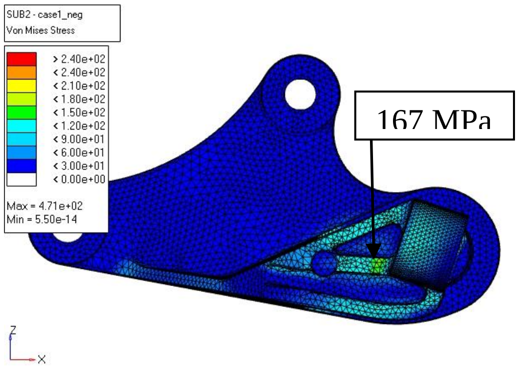

Figure 5.15 : Results of Option2 negative loading condition.

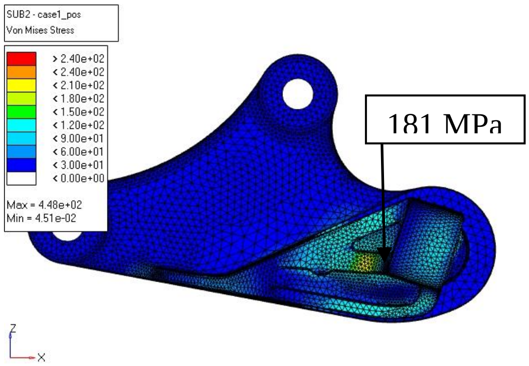

Figure 5.16 : Results of Option3 positive loading condition.

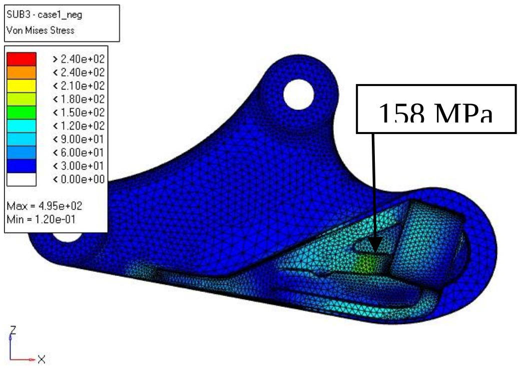

Figure 5.17 : Results of Option3 negative loading condition.

After FEA the stress levels are compared in terms of critical location stress level (seen in Figure 5.12 to Figure 5.17). Increasing radii decreased the regions 2 and 3 stress values significantly. However the region 1 stress value was still not enough to continue (Figure 5.12, Figure 5.13). After increasing radii, thicknesses and heights of ties were also increased additionally in 2nd Option. This design solution decreased region 1 and 4 stress values significantly. However, Von Misses values were increased in regions 2 and 3 (Figure 5.14, Figure 5.15). The 3rd option was presented as both thickness and radii increasing but no wall height increasing. This design solution gave the best results (Figure 5.16, Figure 5.17) in all critical points as referred in Figure 5.10 (see Table 5.2 for results).

Table 5.2 : Von Misses stress values for alternative designs in critical locations as referred in Figure 5.10

Location	Loading	Von Misses Stress [MPa]		
		Option 1	Option 2	Option 3
1	pos	216	179	181
	neg	188	167	158
2	pos	138	146	121
	neg	128	143	114
3	pos	105	127	106
	neg	92	119	95
4	pos	43	23	38
	neg	64	46	59

5.4 Results with design improvement

Optimisation was completed in three numbers of alternative solutions. According to the result after presenting design solutions, selected final shape is Option3 (Figure 5.18). There was %9 weight increasing with this design improvement. NVH is not a critical issue in such a weight increasing, and extra modal analysis is not required for this model.

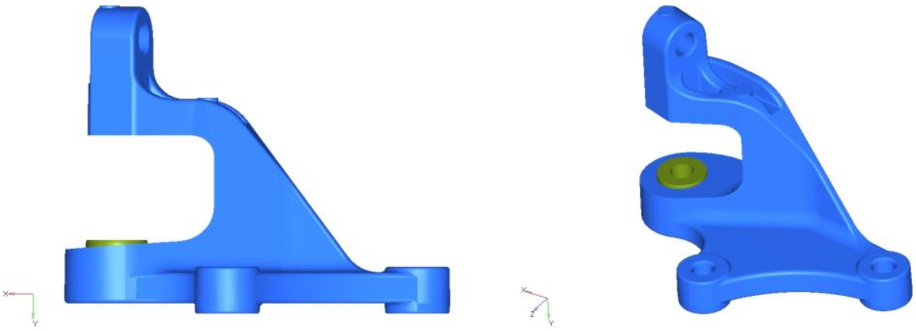

Figure 5.18 : Selected final design after geometry improvement.

New design critical location’s maximum stress value was decreased to 181 MPa. From the S/N curve, it directs that the durability life should be about 200 - 2000 cycles in reversal loading condition. The next step is to confirm the results and correlate the model after re-performing x-direction abuse testing.

6. REPEATED COMPONENT LEVEL ABUSE & TENSILE TESTS

6.1 Static Tensile Test

With respect to tensile durability of TRR bracket for improved design, a static tensile testing was re-performed with five prototypes with same procedure in Gölcük Plant Test Centre. These tests would provide a comparison of the performances of the bracket geometry design in terms of tensile loading. The expected minimum load to failure is 50 kN. As a result, alternative supplier’s all prototypes were passed from static tensile loading according to Ford TRR Bracket Engineering Specification (2004). Please see table for results.

Table 6.1 : Static tensile test results for all production and prototype parts

Supplier	Level	Failure Load	Status
Alternative	Final	50.53 kN	Passed
Alternative	Final	54.33 kN	Passed
Alternative	Final	55.64 kN	Passed
Alternative	Final	57.03 kN	Passed
Alternative	Final	47.56 kN	Passed (-%5)

For the failure location please see Figure 6.1.

Figure 6.1 : Alternative supplier's improved design prototypes photographs after static tensile testing.

6.2 X-Direction Abuse Test

To determine whether alternative supplier's TRR bracket would perform adequately after geometry improvement on CAE, x-direction abuse testing were re-performed with the same procedure in Gölcük Plant Test Centre. These tests would provide a comparison of the performances of the bracket geometries in terms of low cycle fatigue under high impact load.

Four prototype brackets were taken from alternative supplier. The tests were suspended at 2000 cycles if no failure occurred or could be suspended manually in case of any unexpected condition happening.

As a result, all alternative supplier prototypes were passed the testing. The failure region was same with FEA result (Figure 6.2).

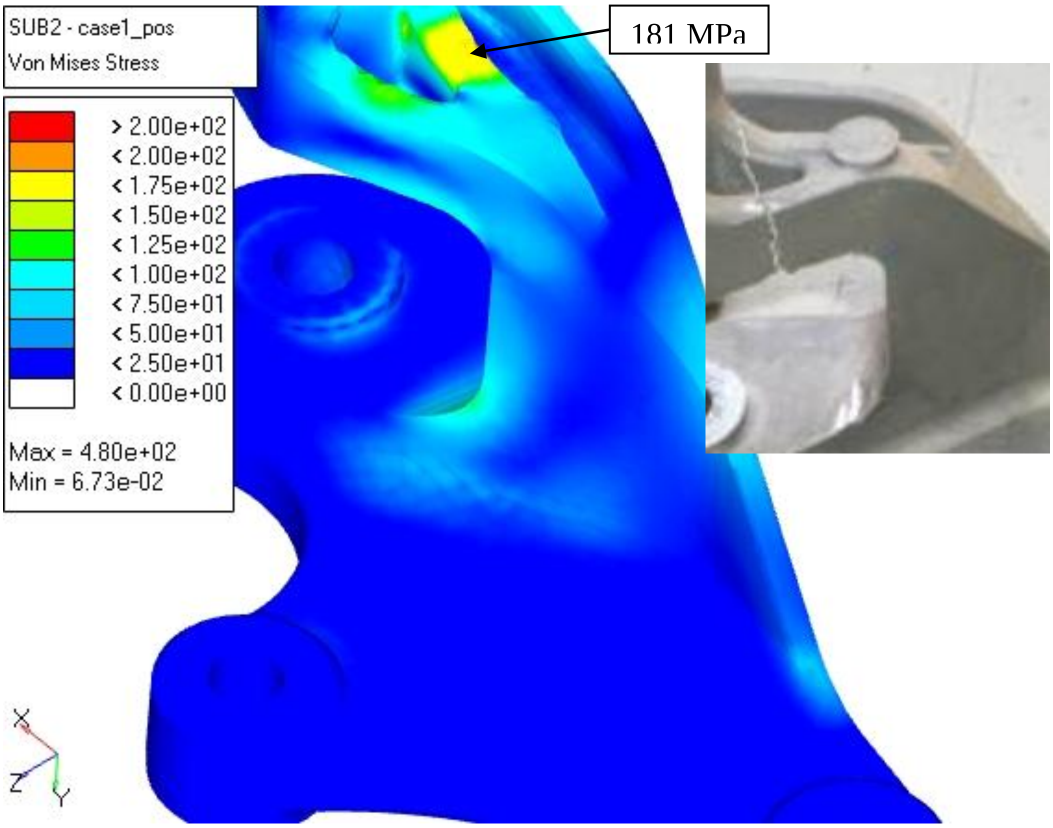

Figure 6.2 : Improved design prototype crack after repeated x-direction abuse testing.

The alternative supplier's test results are shown in Table 6.2.

Table 6.2 : X-direction abuse testing results for all production and prototype parts

Supplier	Level	Failure cycle	Status
Alternative	Final	195 cycle	Passed
Alternative	Final	203 cycle	Passed
Alternative	Final	250 cycle	Passed
Alternative	Final	272 cycle	Passed

6.3 Discussion of the Repeated Testing

As seen in the table average of the life cycle of the parts are between 195-272 cycles. The Von Misses stress value found from FEA was 181 MPa. After integrating the data to SN curves (Figure 6.3) it is seen that the finite element model of the bracket was correlated with the test results. FEA stress resuts correlation is shown on SN curve for alternative supplier initial x-direction abuse testing results (red colored) and re-performed x-direction abuse testing results (cyan colored).

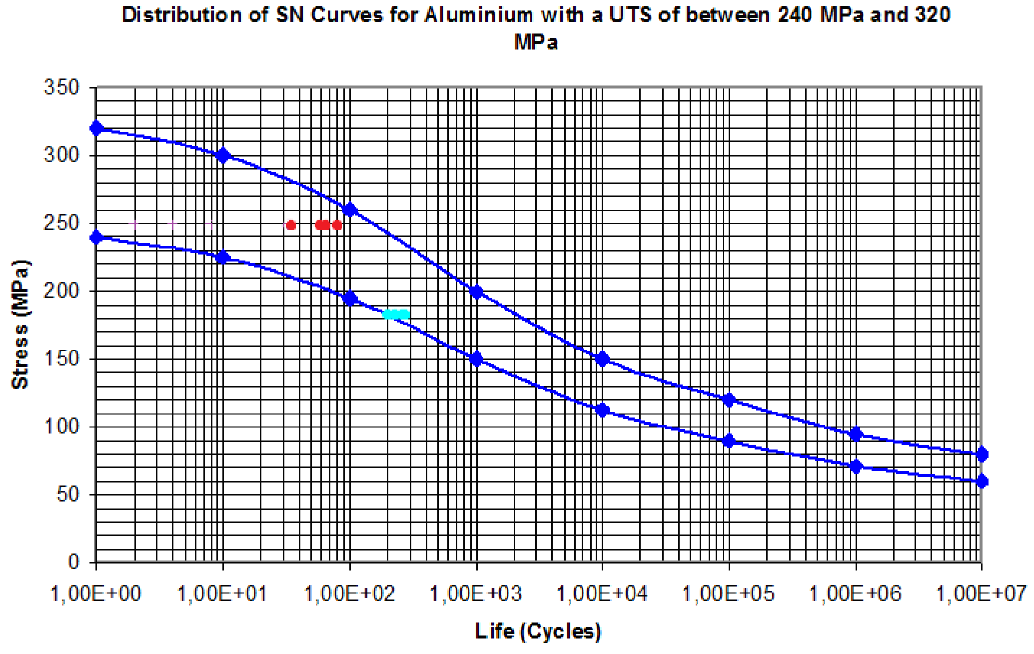

Figure 6.3 : Repeated testing resuts and FEA stress resuts correlation on S/N curve for alternative supplier first results (red colored) and re-performed test results (cyan colored).

Moreover, in terms of tensile load durability, 27 percentage of improvement was seen due to the geometry optimization (Figure 6.4 and Figure 6.5).

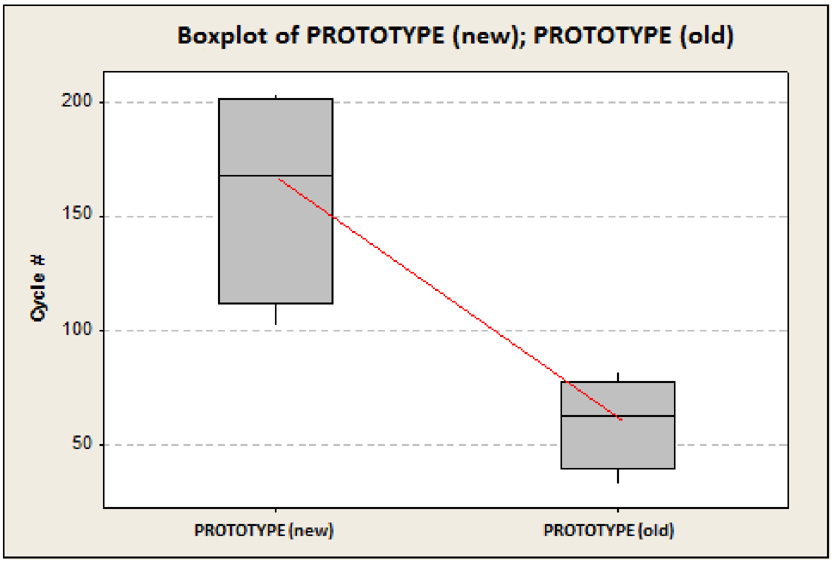

Figure 6.4 : Box plot of the x-direction abuse load testing results comparison of alternative supplier parts before and after geometry improvement.

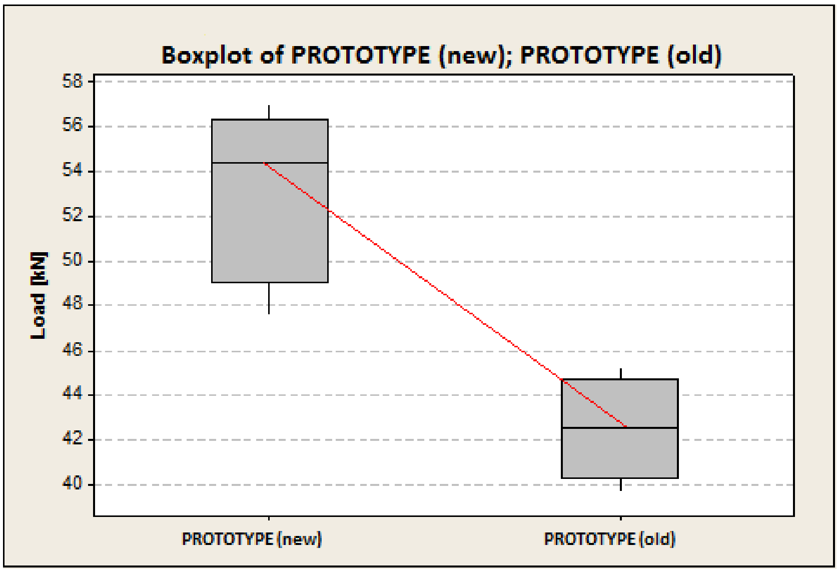

Figure 6.5 : Box plot of the static tensile testing results comparison of alternative supplier parts before and after geometry improvement.

As referenced to the results Driveline Impact & Snap Start Testing as a vehicle level testing was skipped to gain time and money.

7. NEXT STEPS OF THE STUDY

In this chapter, Altair OptiStruct Topology Optimisation tool is used as a weight reduction optimisation with the correlated model is performed without performing any vehicle level testing. Only cheap rig testing with less number of samples are enough to sign-off the parts in a short time interval for implementation as a next step.

It is a high risk to optimize a part without understanding the system in detail (loads, boundary conditions and targets). Topology optimization gives a design proposal which has to be transferred into a feasible design with respect to die-cast process using topology optimization systematically for all castings requires efficient simulation process and data management. Advantages using topology optimization systematically are averaged weight reduction of 15% compared to non-optimized parts, prediction whether part requirements can be achieved before design process in CAD-system is initiated, and reduction of development time by releasing die-cast tools based on simulation results as Hougardy (2009) mentioned in 3rd European HyperWorks Technology Conference.

7.1 Topology Optimisation Model and Results

For the bracket meshing, constraint and forces definitions, and all procedures are same for the FE modelling that was built the previous section and was correlated with testing results.

The optimisation design volume (Figure 7.1) was assigned with aluminium properties. Selected design variable constraint with displacement level of the force application point. The upper bound did have the same value with the final design solution displacement value (0.02mm). For the manufacturing capability to produce the final solution, draw direction and non-design volume as an obstacle were selected. There was volume response for the model to define design volume. Constraint was bounded with volume response with minimum displacement value.

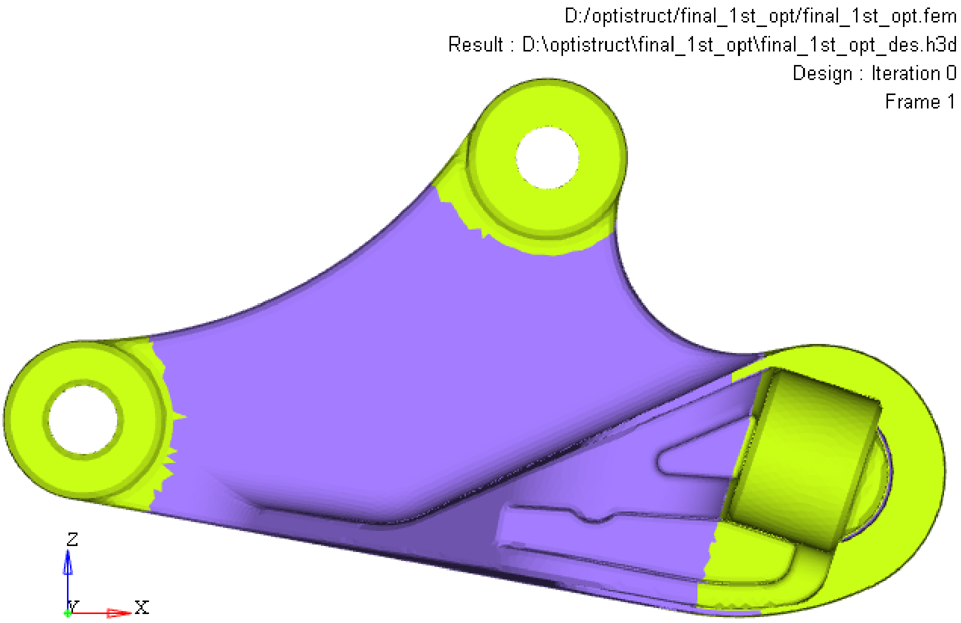

Figure 7.1 : Optimisation design (violet coloured) and non-design (yellow coloured) areas.

For the analyse output, stress and strain card are selected. Before the model was sent to analyse, optistruct checking module was used to see whether there is any problem with model or assigned parameters. After all checking are completed, analyse was completed with 11th number of iterations (Figure 7.2).

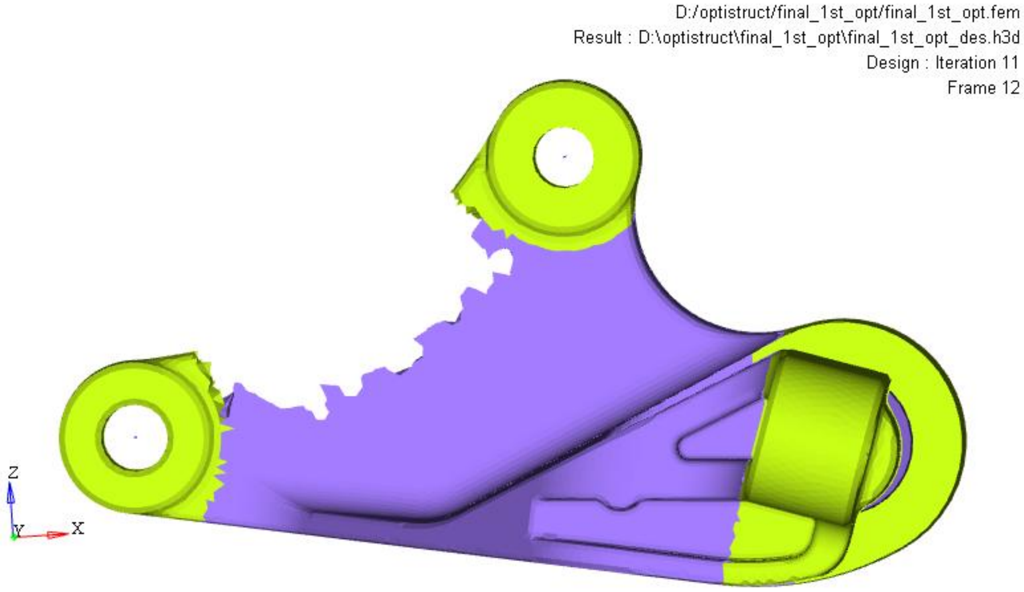

Figure 7.2 : Design solution of OPTISTRUCT after 11th number of iterations.

This design is still in concept phase and should be improved according to roughness and looking respect. A new design (Figure 7.3 and Figure 7.4) that will be able to manufacturing should be still in the safe side according to the Von Misses stresses.

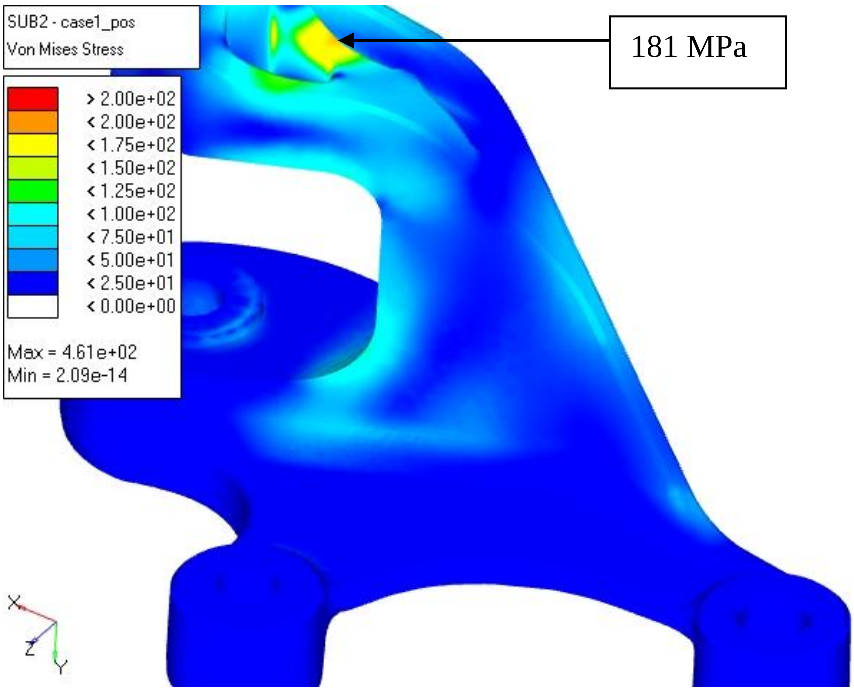

Figure 7.3 : Optimised bracket stress levels in positive loading condition.

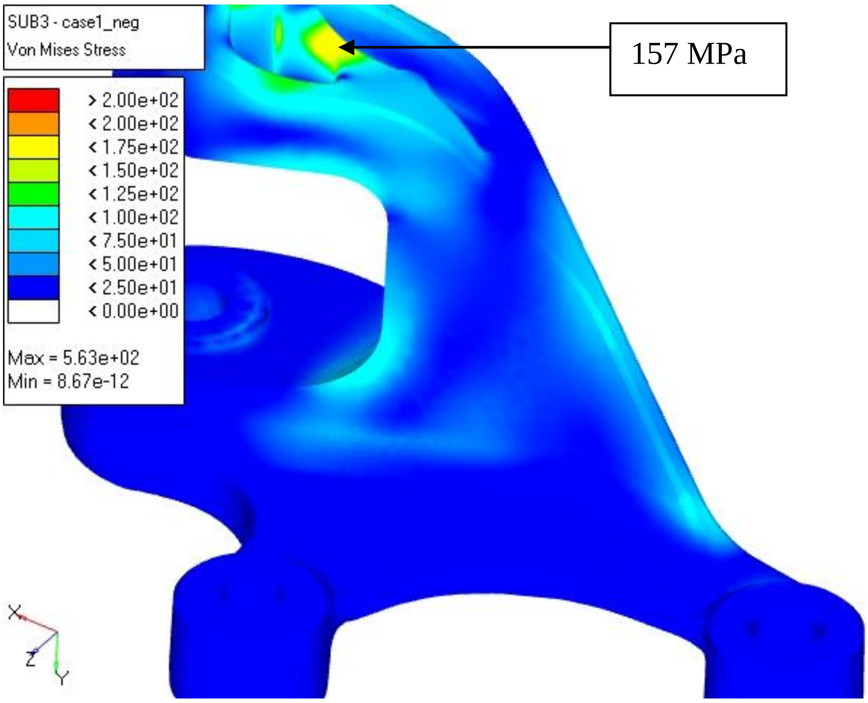

Figure 7.4 : Optimised bracket stress levels in negative loading condition.

The same procedure was followed while performing FEA to optimised bracket. All force and boundary conditions are same. For the FEA results please see Table 7.1.

Table 7.1 : Von Misses stress values for optimised design in critical locations as referred in Figure 5.10

Location	Loading	Von Misses Stress [MPa]	
		Optimised Design	Improved Design
1	Positive	181	181
	Negative	157	158
2	Positive	120	121
	Negative	112	114
3	Positive	107	106
	Negative	96	95
4	Positive	37	38
	Negative	60	59

By optimizing, 10 % weight reduction would be provided with the same Von Misses stress values. All testing expenses, material cost and engineering time consumption were decreased by this study.

8. SUMMARY AND CONCLUSION

As a summary, TRR bracket failures, main reasons of failure modes were investigated and problem was solved by improving TRR bracket design.

Before start investigation of failure modes, TRR bracket design or process history and warranty data reviewed to understand failure mode well. In this manner the first important data was the failures were focused on low mileage that refers generally the impact load failures.

As defining the failure modes; Assembly line process, current production parts and alternative suppliers' prototypes material and geometry of the bracket were reviewed. In assembly line process, bolt torque process capability was investigated and studied by the help of Weilbull diagrams that show no problem with line process.

To eliminate the effects of material properties, chemical composition, and hardness analysis have done for each supplier. All material properties were in specifications.

To eliminate manufacturing process porosity analysis were conducted. For the alternative supplier Level 1 and Level 2 referenced to ASME 505 specifications were satisfied. Although the current supplier was signed off before, the porosity was detected while conducting testing. This was resulted with worse testing results.

To simulate the real road condition of the vehicle, vehicle durability test, driveline impact test and comparison oriented abuse & static tests are performed with the new supplier TRR bracket designs. As seen x-direction abuse test (component level) is correlated with Driveline Impact & Snap Start Testing, FEM was built referenced to x-direction abuse testing. According to the testing results and FEA, modifications on increasing radii & thickness of supports were studied as the proposals for improvement. Several Finite Element Analyses were performed for each proposal. The results of the analyses were compared with the vehicle and component test results, which were performed during TRR bracket improvement studies. Thanks to improvement study, Ford TRR Bracket Engineering Specification (2004) was achieved and 27 percent of improvement was achieved in tensile loading.

In addition to design improvement of the TRR bracket, weight optimization was performed with correlated FEM, as a next step of the study. All testing expenses, material cost and engineering time consumption were decreased significantly.

REFERENCES

Aichberger W., Riener H., Dannbauer H., 2007: Regarding Influences of Production Processes on Material Parameters in Fatigue Life Prediction, *SAE 2007 World Congress*, Magna Powertrain Engineering Centre, Detroit.

Basquin O. H., 1910: The Exponential Law of Endurance Tests, Proc. ASTM, Vol. 10, Part II, ASTM, West Conshochoken, PA, 1910, p. 625.

Dubensky R.G., 1986: What Every Engineer Should Know About Finite Element Analysis Methods, *SAE*, 861294, Chrysler Motors Corp.

Farrington K., Hansen M., Kitto G., Sykes M., Wilson I., 2003: Modelling, Analysis and Reporting Guidelines, Ford Motor Company, 6th October

Ford TRR Bracket Engineering Specification, 2004: Ford Motor Company, Dunton

Hougardy, P., 2009: Topology optimization of engine and gearbox mount castings, *3rd European HyperWorks Technology Conference*, AUDI AG, Ludwigsburg.

Juvinall R.C. and Marshek K. M., 1991: Fundamentals of Machine Component Design, *John Wiley and Sons,* New York.

Kenneth H. Huebner, Earl A. Thornton, 1982: Finite Element Method for Engineers, *John Wiley & Sons*, New York.

Norm, 2007: Bağlantı Elemanları Teknik Eğitim Kataloğu.

P/T Mounts Design Review, 2004: Ford Motor Company, Dunton

P/T Mount System Design Guideline, 2004: Ford Motor Company, Dunton

Turner M. J., Clough R. W., Martin H. C. and Topp L. J., 1956: Stiffness and Deflection Analysis of Complex Structures, *J. of Aero. Sci*., 23 (9).

Wilson, J. Ian, 2004: Correlation of CAE and component rig test results in High Pressure Die Cast Aluminium for use in Powertrain Mounting Systems, *Final Report,* Department of Aeronautical & Automotive Engineering, Loughborough University.

Please Note – All internal documents are confidential, Ford documents retained on the internal Ford European Powertrain Mounts web site. If required, they may be obtained through Kevin Farrington.

APPENDICES

APPENDIX A : Tables
APPENDIX B : Figures

APPENDIX A

Table A.1 : Chemical properties of EN AC-46000 and EN AC- 46200 in British Standard EN 1706:1998

Table 1 — Chemical compositions of casting alloys (expressed in percentage by mass) *(continued)*

Alloy group	Alloy designation		Chemical composition in % by mass													
	Numerical	Chemical symbols	Si	Fe	Cu	Mn	Mg	Cr	Ni	Zn	Pb	Sn	Ti	Others[1)] Each	Others[1)] Total	Aluminium
AlSi5Cu	EN AC-45000	EN AC-Al Si6Cu4	5,0 to 7,0	1,0 (0,9)	3,0 to 5,0	0,20 to 0,65	0,55	0,15	0,45	2,0	0,30	0,15	0,25 (0,20)	0,05	0,35	Remainder
	EN AC-45100	EN AC-Al Si5Cu3Mg	4,5 to 6,0	0,60 (0,50)	2,6 to 3,6	0,55	0,15 to 0,45 (0,20 to 0,45)	—	0,10	0,20	0,10	0,05	0,25 (0,20)	0,05	0,15	Remainder
	EN AC-45200	EN AC-Al Si5Cu3Mn	4,5 to 6,0	0,8 (0,7)	2,5 to 4,0	0,20 to 0,55	0,40		0,30	0,55	0,20	0,10	0,20 (0,15)	0,05	0,25	Remainder
	EN AC-45300	EN AC-Al Si5Cu1Mg	4,5 to 5,5	0,65 (0,55)	1,0 to 1,5	0,55	0,35 to 0,65 (0,40 to 0,65)	—	0,25	0,15	0,15	0,05	0,05 to 0,25 (0,05 to 0,20)	0,05	0,15	Remainder
	EN AC-45400	EN AC-Al Si5Cu3	4,5 to 6,0	0,60 (0,50)	2,6 to 3,6	0,55	0,05	—	0,10	0,20	0,10	0,05	0,25 (0,20)	0,05	0,15	Remainder
AlSi9Cu	EN AC-46000	EN AC-Al Si9Cu3(Fe)	8,0 to 11,0	1,3 (0,6 to 1,1)	2,0 to 4,0	0,55	0,05 to 0,55 (0,15 to 0,55)	0,15	0,55	1,2	0,35	0,25	0,25 (0,20)	0,05	0,25	Remainder
	EN AC-46100	EN AC-Al Si11Cu2(Fe)	10,0 to 12,0	1,1 (0,45 to 1,0)	1,5 to 2,5	0,55	0,30	0,15	0,45	1,7	0,25	0,25	0,25 (0,20)	0,05	0,25	Remainder
	EN AC-46200	EN AC-Al Si8Cu3	7,5 to 9,5	0,8 (0,7)	2,0 to 3,5	0,15 to 0,65	0,05 to 0,55 (0,15 to 0,55)	—	0,35	1,2	0,25	0,15	0,25 (0,20)	0,05	0,25	Remainder
	EN AC-46300	EN AC-Al Si7Cu3Mg	6,5 to 8,0	0,8 (0,7)	3,0 to 4,0	0,20 to 0,65	0,30 to 0,60 (0,35 to 0,60)	—	0,30	0,65	0,15	0,10	0,25 (0,20)	0,05	0,25	Remainder
	EN AC-46400	EN AC-Al Si9Cu1Mg	8,3 to 9,7	0,8 (0,7)	0,8 to 1,3	0,15 to 0,55	0,25 to 0,65 (0,30 to 0,65)	—	0,20	0,8	0,10	0,10	0,10 to 0,20 (0,10 to 0,18)	0,05	0,25	Remainder
	EN AC-46500	EN AC-Al Si9Cu3(Fe)(Zn)	8,0 to 11,0	1,3 (0,6 to 1,2)	2,0 to 4,0	0,55	0,05 to 0,55 (0,15 to 0,55)	0,15	0,55	3,0	0,35	0,25	0,25 (0,20)	0,05	0,25	Remainder
	EN AC-46600	EN AC-Al Si7Cu2	6,0 to 8,0	0,8 (0,7)	1,5 to 2,5	0,15 to 0,65	0,35	—	0,35	1,0	0,25	0,15	0,25 (0,20)	0,05	0,15	Remainder
AlSi(Cu)	EN AC-47000	EN AC-Al Si12(Cu)	10,5 to 13,5	0,8 (0,7)	1,0 (0,9)	0,05 to 0,55	0,35	0,10	0,30	0,55	0,20	0,10	0,20 (0,15)	0,05	0,25	Remainder
	EN AC-47100	EN AC-Al Si12Cu1(Fe)	10,5 to 13,5	1,3 (0,6 to 1,1)	0,7 to 1,2	0,55	0,35	0,10	0,30	0,55	0,20	0,10	0,20 (0,15)	0,05	0,25	Remainder

Table A.2 : Mechanical properties of EN AC-46000 and EN AC- 46200 in British Standard EN 1706:1998

Table A.1 — Mechanical properties of pressure die cast alloys (see 6.3.2.5)

Alloy group	Alloy designation		Temper	Tensile strength	Proof stress	Elongation	Brinell hardness
	Numerical	Chemical symbols	Designation	R_m MPa min.	$R_{p0,2}$ MPa min.	A_{50mm} % min.	HBS min.
AlSi10Mg	EN AC-43400	EN AC-Al Si10Mg(Fe)	F	240	140	1	70
AlSi	EN AC-44300	EN AC-Al Si12(Fe)	F	240	130	1	60
	EN AC-44400	EN AC-Al Si9	F	220	120	2	55
AlSi9Cu	EN AC-46000	EN AC-Al Si9Cu3(Fe)	F	240	140	< 1	80
	EN AC-46100	EN AC-Al Si11Cu2(Fe)	F	240	140	< 1	80
	EN AC-46200	EN AC-Al Si8Cu3	F	240	140	1	80
	EN AC-46500	EN AC-Al Si9Cu3(Fe)(Zn)	F	240	140	< 1	80
AlSi(Cu)	EN AC-47100	EN AC-Al Si12Cu1(Fe)	F	240	140	1	70
AlMg	EN AC-51200	EN AC-Al Mg9	F	200	130	1	70

1 N/mm^2 = 1 MPa

APPENDIX B

PARÇA ADI *PART NAME*	TRANS BRKT-ROLL RESTRICTOR	PARÇA NO. *PART NO.*	-6P093-
İMALATÇI *SUPPLIER*		TARİH *DATE* 10.09.2009	NUMUNE ADEDİ *NO. OF SAMPLES* 2

SIRA NO. *ITEM NO.*	KARAKTER BOYUT SPESİFİKASYON *CHARACTERISTIC DIM.SPEC.*	KONTROL SONUÇLARI *RESULT OF CONTROL*	
		1.PARÇA	2.PARÇA
	SERTLİK:80 HB. Min.	102 HB	104 HB
		106 HB	106 HB
		104 HB	105 HB
		105 HB	105 HB
		102 HB	104 HB
		104 HB	103 HB
		105 HB	104 HB
	MALZEME ANALİZİ		
	EN 1706		
	%Si: 8.0 - 11.00	% 10.1	
	%Fe:1.3 max:(0.6-1.1)	% 1.2	
	%Cu:2.0 - 4.0	% 4.0	
	%Mn:0.55 max.	% 0.27	
	%Mg:0.05-0.55	Spectrometre Mg. Ölçemiyor.	
	%Cr:0.15 max.	% 0.02	
	%Ni:0.55 max.	% 0.07	
	%Zn:1.2 max.	% 1.05	
	%Pb:0.35 max.	% 0.07	
	%Sn:0.25 max.	% 0.04	
	%Ti:0.25 max.	% 0.02	
		ÖLÇÜM YAPILAN CİHAZLAR : 402-190	

Figure B.1 : Chemical and mechanical properties testing results of production parts (EN AC-46200).

PARÇA ADI *PART NAME*	TRANS BRKT-ROLL RESTRICTOR	PARÇA NO. *PART NO.*	[redacted] -6P093- [redacted]
İMALATÇI *SUPPLIER*	[redacted]	TARİH *DATE* 10.09.2009	NUMUNE ADEDİ *NO.OF SAMPLES* 2

SIRA NO. *ITEM NO.*	KARAKTER BOYUT SPESİFİKASYON *CHARACTERISTIC.DIM.SPEC.*	KONTROL SONUÇLARI *RESULT OF CONTROL*	
		1.PARÇA	**2.PARÇA**
	SERTLİK:80 HB. Min.	106 HB	107 HB
		105 HB	104 HB
		104 HB	105 HB
		105 HB	108 HB
		107 HB	104 HB
		104 HB	105 HB
		106 HB	104 HB
	MALZEME ANALİZİ		
	EN 1706-EN AC 46000 AlSi9Cu		
	%Si: 8.0 - 11.00	% 8.5	
	%Fe:1.3 max.(0.6-1.1)	% 0.85	
	%Cu:2.0 - 4.0	% 3.6	
	%Mn:0.55 max.	% 0.22	
	%Mg:0.05-0.55	Spectrometre Mg. Ölçemiyor.	
	%Cr:0.15 max.	% 0.03	
	%Ni:0.55 max.	% 0.07	
	%Zn:1.2 max.	% 1.19	
	%Pb:0.35 max.	% 0.09	
	%Sn:0.25 max.	% 0.02	
	%Ti:0.25 max.	% 0.04	
		ÖLÇÜM YAPILAN CİHAZLAR : 402-190	

Figure B.2 : Chemical and mechanical properties testing results of prototype parts (EN AC-46000).

CURRICULUM VITA

Candidate's full name: Pınar Feyza TOPRAK

Place and date of birth: Ankara, 19.05.1984

Permanent Address: Selimiye Hamam Sk. NO: 53/4
Üsküdar / İstanbul

Universities and Colleges attended: Middle East Technical University (Bachelor's)
İstanbul Technical University (M.Sc.)